

Hydrogen-like ions in plasma environment

Neetik Mukherjee^{a,*} Chandra N. Patra^{b,†} and Amlan K. Roy^{a,‡}

^a*Department of Chemical Sciences, IISER Kolkata,*

Mohanpur-741246, Nadia, WB, India

^b*Theoretical Chemistry Section, Chemistry Group,*

Bhabha Atomic Research Centre, Mumbai-400085, India

Abstract

The behavior of H-like ions embedded in astrophysical plasmas in the form of *dense, strongly and weakly coupled* plasmas are investigated. In these, the increase and decrease in temperature is impacted with a change in confinement radius (r_c). Two independent and generalized scaling ideas have been applied to modulate the effect of plasma screening constant (λ) and charge of ion (Z) on such systems. Several new relations are derived to interconnect the original Hamiltonian and two scaled Hamiltonians. In exponential cosine screened Coulomb potential (ECSCP) (dense) and weakly coupled plasma (WCP) these scaling relations have provided a linear equation connecting the critical screening constant ($\lambda^{(c)}$) and Z . Their ratio offers a state-dependent constant, beyond which, a particular state vanishes. Shannon entropy has been employed to understand the plasma effect on the ion. With increase in λ , the accumulation of opposite charge surrounding the ion increases leading to a reduction in number of bound states. However, with rise in ionic charge Z , this effect can be delayed. The competing effect of plasma charge density (n_e) and temperature in WCP and ECSCP is investigated. A recently proposed simple virial-like theorem has been established for these systems. Multipole ($k = 1 - 4$) oscillator strength (OS) and polarizabilities for these are studied considering $1s, 2s$ states. As a bonus, analytical closed-form expressions are derived for $f^{(k)}$ and $\alpha^{(k)}$ ($k = 1 - 4$) involving $1s$ and $2s$ state, for *free H-like ion*.

PACS: 03.65.-w, 03.65.Ca, 03.65.Ge, 03.65.Db.

Keywords: Plasma environment, virial theorem, oscillator strength, polarizabilities

*Electronic address: pchem.neetik@gmail.com

†Electronic address: patra@barc.gov.in

‡Corresponding author. Email: akroy@iiserkol.ac.in, akroy6k@gmail.com.

I. INTRODUCTION

The discovery and development of quantum confinement [1] has triggered the study of influence of environment on quantum systems. In confined condition, rearrangement of orbitals may occur in atoms/molecules, leading to some fascinating changes in physical, chemical properties. Especially this leads to an increase in coordination number of atoms [2], enhanced reactivity of atoms/molecules, room temperature superconductivity [3], etc. The environment driven confinement has profound application in condensed matter, semiconductor physics, astrophysics, nanotechnology etc. In this context, the influence of plasma environment [4–6] in astrophysical systems is a subject of topical interest. Particularly, the impact of charge cloud and temperature on bound quantum states can be determined by investigating atoms and ions trapped inside various plasma environments [7–9].

In such conditions, the competing effect of plasma free electron density (n_e) and temperature (T) play a pivotal role in stabilizing the bound states of a given system. The plasma coupling parameter (Γ) is expressed as [10];

$$\Gamma = \frac{E_{\text{coulomb}}}{E_{\text{thermal}}} = \frac{Q^2}{4\pi\epsilon_0 a k_b T}. \quad (1)$$

Here, Q denotes the charge on the particle, inner particle separation is given by $a = \left(\frac{3}{4\pi n_e}\right)^{\frac{1}{3}}$, k_b signifies Boltzmann constant, and n_e refers to plasma electron density. Depending on the value of Γ , following two situations may be envisaged.

1. $\Gamma < 1$: This arises for low dense and high temperature or weakly coupled plasma (WCP). The thermal energy is higher than coulomb energy in this case.
2. $\Gamma > 1$: This occurs for strongly coupled plasma (SCP). They have high density and low temperature. The thermal energy is now lower than coulomb energy. This type of plasma has been produced experimentally.

In hot WCP, the collective screening effect of plasma on the electron-charged particle interaction is assumed to behave as Debye-Hückel potential, expressed in the form, $V_1(r) = -\frac{Z}{r}e^{-\lambda_1 r}$. Here, $\lambda_1 = \sqrt{\frac{4\pi e^2 n_e}{k_b T}}$ corresponds to the inverse of Debye radius (D). The screening parameter arises due to surrounding plasma cloud. In last two decades, this system has been studied vigorously with immense interest. The impact of plasma screening effect on energy spectrum [11–14], inelastic electron-ion scattering [15, 16], two proton transitions

[17, 18] and transition probabilities involving electron-impact excitation [19–21], etc., have been investigated. The dynamic plasma screening effect was considered in [22–25]. The relativistic correction on plasma screening effect was also explored [26]. Various spectroscopic properties including multipole oscillator strength (OS) and static multipole polarizabilities were calculated for H-like atoms embedded in WCP [27–31] using several numerical methods. A time-dependent variation perturbation method was employed to calculate transition probabilities, OS, static dipole polarizabilities for ground state at different λ_1 values [32]. Numerical symplectic integration method [28–30], mean excitation energy based approximation formula [31], integration based shooting technique [33], linear variation method [34], etc., were also employed to extract these spectroscopic properties. The hyperpolarizability of H atom under spherically confined Debye plasma was reported in [35]. Closed form expression for critical screening constant in ground state of WCP was proposed in [36]. Numerical values for ground and low-lying excited states were reported in [37]. Recently, generalized pseudo spectral (GPS) method was used in computing OS and polarizabilities in ground and excited states ($\ell = 0$) [7]. In all these cases, calculations were mostly concentrated in estimating the dipole OS and polarizabilities considering $1s$ as the initial state. However, WCP in a *confined* condition with varying λ_1 has not yet been well explored. This remains one of the primary objectives of this communication.

The composite screening and wake effect around a slow moving test charge in low density quantum plasma is mimicked by using an exponential cosine screened Coulomb potential (ECSCP), having the form, $V_2(r) = -\frac{Z}{r}e^{-\lambda_2 r} \cos \lambda_2 r$. Here, $\lambda_2 = \frac{k_q}{\sqrt{2}} = \sqrt{\frac{n_e \omega_{pe}}{\hbar}}$ signifies the screening parameter, whereas k_q is the electron plasma wave number connected to electron plasma frequency and number density. The cosine term in this model is introduced under the assumption that the quantum force acting on plasma electrons predominates over statistical pressure of plasmas [9]. A variety of theoretical methods like perturbation and variation method [38], Padé scheme [39], shooting method [40], SUSY perturbation method [41], asymptotic iteration [42], variation using hydrogenic wave functions [43], J-matrix [44], symplectic integration [45], GPS [46], basis expansion method with Slater-type orbitals [47], Laguerre polynomials [48], etc, were employed to extract the eigenvalue and eigenfunctions of this system. Similarly, the influence of λ_2 on energy spectrum [13, 14], electron-impact excitation [21], photoionization cross-section [48, 49], etc., were discussed in appreciable detail. Relativistic correction to the screening effect was also explored. Further, the laser-

induced excitation on confined H atom (CHA) in ECSCP was pursued using Bernstein-polynomial method [50]. In this context, the impact of shape of laser pulse, r_c , λ_2 , as well as various laser parameters on the dynamics of the system has been examined and analyzed. Several attempts were made to estimate the characteristic value of λ_2 at which a bound state designated by quantum numbers n, ℓ disappears [36]. The critical screening parameters for $n \leq 6$ and $0 \leq \ell \leq n - \ell$ was accurately estimated in [51]. The dipole OS and polarizabilities at various λ_2 values were reported before in [40, 41, 45, 47, 52]. Recently, the utility of GPS method in ECSCP [9] has been examined by evaluating OS and polarizabilities. But here again, barring a few exceptions, majority calculations have focused in ground state. Moreover, to the best of our knowledge, ECSCP under a *confined* environment has not been probed so far in a sufficiently thorough manner.

In SCP [4], an ion experiences plasma effect within the ion sphere radius (R). Thus, no electron current moves through the boundary surface. It is generally described by a potential of the form [33],

$$V_3(r) = \begin{cases} = -\frac{Z}{r} + \left(\frac{Z-N_e}{2R}\right) \left[3 - \left(\frac{r}{R}\right)^2\right] \\ = 0 & r > r_c = R, \end{cases} \quad (2)$$

where $R = \left[\frac{3(Z-N_e)}{4\pi n_e}\right]^{\frac{1}{3}}$. The free electrons in an ion sphere distribute uniformly. This model is extensively used and expected to be valid in the limit of low temperature and high density. Several theoretical methods have been employed to understand the effect of SCP on energy levels and wave functions of H-like atoms [53–55]. Moreover, atomic transition probabilities [56], transition energies and polarizabilities [33], photoionization and photoionization cross section [10, 57], OS and static polarizabilities [58], etc., in this case, were studied previously. However, akin to the earlier two cases (WCP and ECSCP), most of the works have been restricted to ground state only.

We have a number of objectives in this article. At first, a detailed investigation is made on the three plasma conditions, *viz.*, WCP, ECSCP and SCP, with special emphasis on their confinement situation and excited states, where, literature results are quite scarce. It may be noted that, the influence of a physical situation governed by a potential of the form, $V = \infty$, at $r > r_c$, in the context of plasma has not been considered before. Besides, its significance and relation to the plasma environment is also not very clear. Here the confined condition is mapped with *plasma temperature*. It may be noted that, the multipole OS and

polarizabilities of H atom in various plasmas have been reported in a number of publications. However, such works in the confined scenario, as implied above, have not been considered before. Thus a secondary objective is to examine the *effect of confinement* on multipole OS and polarizabilities for WCP, ECSCP and SCP. Two different scaling ideas connecting λ and Z are formulated. The relation between these two individual concepts are derived and explained. Additionally, Shannon entropy (S) has been invoked to determine the critical screening constant in *free* WCP and ECSCP. This has been attempted for the first time and our results show this can be an interesting and novel route. Beyond this critical parameter (the binding energy of a given state disappears), no bound states could be found. After some debate, It is now a well accepted fact that, the standard form of virial theorem (VT) does not ordinarily obey in enclosed conditions. An appropriate modified form is invoked in [59], which holds good in both free and confined conditions. The utility and efficiency of this newly derived relation is examined in the context of plasma environment.

Thus we have performed detailed calculations of multipole OS ($k = 1 - 4$) and polarizabilities in $1s$, $2s$ states of WCP, ECSCP and SCP employing the accurate GPS wave functions. Here $k = 1 - 4$ represent dipole, quadrupole, octupole and hexadecapole transitions respectively. In WCP and ECSCP, we have demonstrated the spectroscopic properties in two different ways. At first, these are calculated by varying λ , keeping r_c fixed. Secondly, the impact of variation of r_c on these properties at fixed λ is also verified. Analogous calculations are done in SCP, with change in r_c . As a bonus, some analytical closed-form expressions of multipole OS (up to hexadecapole) and polarizabilities (up to hexadecapole) are derived for $1s$, $2s$ states of *free H atom* (FHA). In literature, these forms are available in *dipole case only*. The article is organized in following parts: Sec. II presents a brief description about the formalism employed in the current work. In Section III, the connection between plasma temperature and quantum confinement is proposed and explained. Section IV provides a detailed discussion of the results for WCP, ECSCP and SCP. Finally, we conclude with a few remarks and future prospects, in Sec. V.

II. THEORETICAL FORMALISM

The time-independent radial Schrödinger equation (SE) for the spherically confined plasma system is expressed as (in a.u.),

$$\left[-\frac{1}{2} \frac{d^2}{dr^2} + \frac{\ell(\ell+1)}{2r^2} + V_c(r) + V_0 \theta(r-r_c) \right] \psi_{n,\ell}(r) = \mathcal{E}_{n,\ell} \psi_{n,\ell}(r). \quad (3)$$

Here V_0 is a positive number with numerical value approaching ∞ and $\theta(r-r_c)$ is a Heaviside function that reaches 1 at $r = r_c$, while *zero* otherwise, whereas $V_c(r)$ represents the various plasma potential discussed later in this section. To calculate energy and spectroscopic properties, the GPS method has been exploited. Over the time, its accuracy and efficiency in calculating various bound-state properties in several central potentials in both free and confined condition have been verified and established (see [59–63] and references therein).

A. Virial-like Theorem

Recently a virial-like relation has been proposed for free and confined quantum systems, by invoking the time-independent non-relativistic SE and Hypervirial theorem [59]. The generalized form of this equation is expressed as,

$$\langle \hat{T}^2 \rangle_n - \langle \hat{T} \rangle_n^2 = \langle \hat{V}^2 \rangle_n - \langle \hat{V} \rangle_n^2 \quad (4)$$

It can be used as a necessary condition for an exact quantum system to obey. Further, it has been proved that, the following equation,

$$(\Delta \hat{T}_n)^2 = \langle \hat{V} \rangle_n \langle \hat{T} \rangle_n - \langle \hat{T} \hat{V} \rangle_n = (\Delta \hat{V}_n)^2 = \langle \hat{T} \rangle_n \langle \hat{V} \rangle_n - \langle \hat{V} \hat{T} \rangle_n, \quad (5)$$

can act as a sufficient condition for a bound, stationary state [59]. Moreover, an alteration in boundary condition does not influence the general form. These are applicable in all coordinate systems, such as ellipsoidal, parabolic, cylindrical, spheroidal, etc. This also holds good in unconfined and confined systems (including angular confinement). In the present endeavor, this has been extended to the plasma environment.

B. Multipole polarizabilities

The static multipole polarizabilities can be expressed in following form,

$$\alpha_i^{(k)} = \alpha_i^{(k)}(\text{bound}) + \alpha_i^{(k)}(\text{continuum}). \quad (6)$$

It is customary to write $\alpha_i^{(k)}$ in terms of compact sum-over states form [33]. However it can also be directly computed by adopting the standard perturbation theory framework [64]. In the former procedure, Eq. (5) modifies to,

$$\alpha_i^{(k)} = \sum_n \frac{f_{ni}^{(k)}}{(\mathcal{E}_n - \mathcal{E}_i)^2} - c \int \frac{|\langle R_i | r^k Y_{kq}(\mathbf{r}) | R_{en} \rangle|^2}{(\mathcal{E}_{en} - \mathcal{E}_i)} d\epsilon, \quad (7)$$

$$\alpha_i^{(k)}(\text{bound}) = \sum_n \frac{f_{ni}^{(k)}}{(\Delta\mathcal{E}_{ni})}, \quad \alpha_i^{(k)}(\text{continuum}) = c \int \frac{|\langle R_i | r^k Y_{kq}(\mathbf{r}) | R_{en} \rangle|^2}{(\mathcal{E}_{en} - \mathcal{E}_i)} d\epsilon.$$

In Eq. (6), the summation and integral terms represent the bound and continuum contributions respectively, $f_{ni}^{(k)}$ signifies the multipole OS (k is a positive integer), c is a constant which depends on ℓ quantum number. $f_{ni}^{(k)}$ measures the mean probability of transition between an initial (i) to final (n) state, which is normally expressed as,

$$f_{ni}^{(k)} = \frac{8\pi}{(2k+1)} \Delta\mathcal{E}_{ni} |\langle r^k Y_{kq}(\mathbf{r}) \rangle|^2. \quad (8)$$

Designating the initial and final states as $|n\ell m\rangle$ and $|n'\ell' m'\rangle$, one can easily derive,

$$f_{ni}^{(k)} = \frac{8\pi}{(2k+1)} \Delta\mathcal{E}_{ni} \frac{1}{2\ell+1} \sum_m \sum_{m'} |\langle n'\ell' m' | r^k Y_{kq}(\mathbf{r}) | n\ell m \rangle|^2. \quad (9)$$

The application of Wigner-Eckart theorem and sum rule for $3j$ symbol further leads to,

$$f_{ni}^{(k)} = 2 \frac{(2\ell'+1)}{(2k+1)} \Delta\mathcal{E}_{ni} |\langle r^k \rangle_{n\ell}^{n'\ell'}|^2 \left\{ \begin{matrix} \ell' & k & \ell \\ 0 & 0 & 0 \end{matrix} \right\}^2. \quad (10)$$

The transition matrix element is expresses by the radial integral,

$$\langle r^k \rangle = \int_0^\infty R_{n'\ell'}(r) r^k R_{n\ell}(r) r^2 dr. \quad (11)$$

Thus it is clear that $f_{ni}^{(k)}$ depends on n, ℓ quantum numbers, while being independent of magnetic quantum number m . In this article, we aim to compute multipole ($k = 1 - 4$) polarizabilities and OS for $1s, 2s$ states. The corresponding selection rule for dipole OS ($k = 1$) for these two states are ($i = 1$ or 2),

$$f_{np-is}^{(1)} = 2 \Delta\mathcal{E}_{np-is} |\langle r \rangle_{is}^{np}|^2 \left\{ \begin{matrix} 1 & 1 & 0 \\ 0 & 0 & 0 \end{matrix} \right\}^2 = \frac{2}{3} \Delta\mathcal{E}_{np-is} |\langle r \rangle_{is}^{np}|^2. \quad (12)$$

The quadrupole OS ($k = 2$) can be written as below,

$$f_{nd-is}^{(2)} = 2 \Delta\mathcal{E}_{nd-is} |\langle r^2 \rangle_{is}^{nd}|^2 \left\{ \begin{matrix} 2 & 1 & 0 \\ 0 & 0 & 0 \end{matrix} \right\}^2 = \frac{2}{5} \Delta\mathcal{E}_{nd-is} |\langle r^2 \rangle_{is}^{nd}|^2. \quad (13)$$

Similarly, for the octupole OS ($k = 3$), the expression becomes,

$$f_{nf-is}^{(3)} = 2 \Delta \mathcal{E}_{nf-is} |\langle r^3 \rangle_{is}^{nf}|^2 \left\{ \begin{matrix} 3 & 1 & 0 \\ 0 & 0 & 0 \end{matrix} \right\}^2 = \frac{2}{7} \Delta \mathcal{E}_{nf-is} |\langle r^3 \rangle_{is}^{nf}|^2. \quad (14)$$

And for the hexadecapole OS ($k = 4$), one gets,

$$f_{ng-is}^{(4)} = 2 \mathcal{E}_{ng-is} |\langle r^4 \rangle_{is}^{ng}|^2 \left\{ \begin{matrix} 4 & 1 & 0 \\ 0 & 0 & 0 \end{matrix} \right\}^2 = \frac{2}{9} \Delta \mathcal{E}_{ng-is} |\langle r^4 \rangle_{is}^{ng}|^2. \quad (15)$$

The analytical closed form expressions for multipole oscillator strength ($k = 1 - 4$) for all possible transitions, and polarizabilities in FHA are collected in Appendix A. It is important to mention that, there exists a multipole OS sum rule as follows,

$$S^{(k)} = \sum_m f^{(k)} = k \langle \psi_i | r^{(2k-2)} | \psi_i \rangle, \quad (16)$$

where the summation includes all the bound states.

C. Plasma Characteristics

Plasma is a statistical system of mobile charged particles, which interact with each other through electromagnetic forces. Here, the coupling occurs between quantum states and plasma density. Now we briefly discuss the characteristics of various H-atom plasmas.

In a hot plasma, the collective plasma screening effect on H atom is normally mapped by using Debye-Hückel potential of the form [4],

$$V_1(r) = \begin{cases} = -\frac{Z}{r} e^{-\lambda_1 r}, & r \leq r_c \\ = 0, & r > r_c. \end{cases} \quad (17)$$

In this form of potential, the probability of finding plasma particles inside the Debye sphere is negligible. In addition to screening effect, here it is assumed that the charge cloud is confined in spherical enclosure. This situation provides an alternate boundary condition for such systems. However, at $r_c \rightarrow \infty$ this restriction vanishes. The Debye radius ($D = \frac{1}{\lambda_1}$) plays an important role in WCP. For example (i) at a fixed n_e , $D \propto \sqrt{T}$ and (ii) at a certain T , $D \propto \frac{1}{\sqrt{n_e}}$. Most importantly, at a constant D , $n_e \propto T$. It means that, to keep λ_1 or D fixed, with rise in T , n_e increases. Further, with increase in n_e , the plasma tail

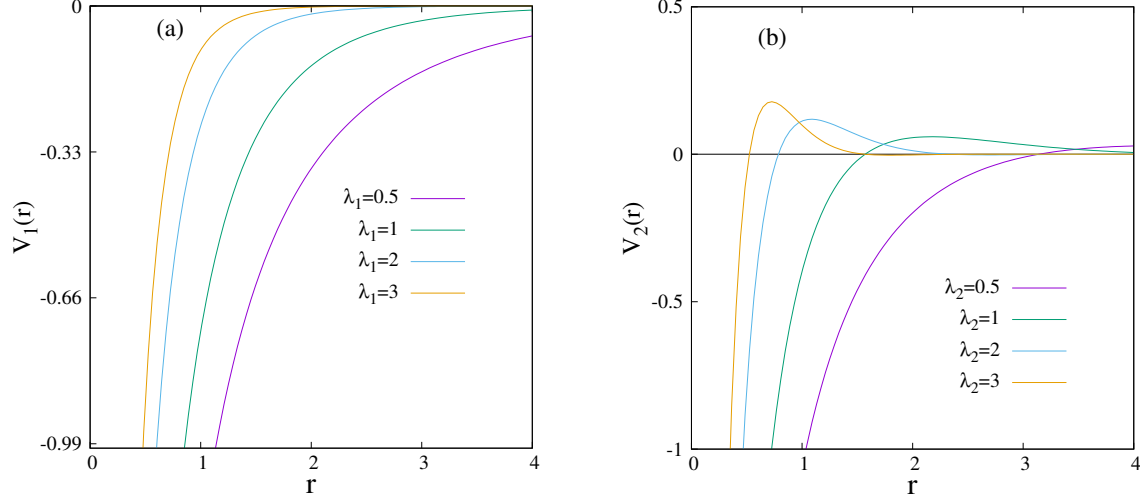


FIG. 1: Plot of (a) $V_1(r)$, Eq. 17 (b) $V_2(r)$, Eq. 18, at selected λ values, namely, 0.5, 1, 2, 3 keeping $Z = 2$. For details, see text.

effect declines. Conversely, with rise in T , it enhances. But, here incorporation of radial confinement indirectly controls the tail effect. When r_c is large, then T predominates over n_e . On the other side, at low r_c region, the effect of n_e prevails. Therefore, in this work, we have probed WCP in two different motives: (i) firstly with the variation of r_c at a fixed λ_1 and (ii) secondly, the effect of λ_1 at a certain r_c . Figure 1(a) portrays that, an enhancement in λ_1 leads to a growth in plasma electron density surrounding the positive ion.

With increase in plasma density, the multi-particle cooperative interaction enhances. Thus, D becomes comparable to de Broglie wave length, and hence quantum effect appears [65]. In this context, Debye-Hückel model becomes inappropriate to explain the plasma properties. In ECSCP, λ_2 is connected to plasma frequency as $\lambda_2 \propto \sqrt{\omega_{pe}}$. It has the form,

$$V_2(r) = \begin{cases} = -\frac{Z}{r} e^{-\lambda_2 r} \cos(\lambda_2 r), & r \leq r_c \\ = 0, & r > r_c, \end{cases} \quad (18)$$

Due to the incorporation of cosine term, ECSCP exhibits stronger screening effect compared to WCP. There occurs a maximum at $r_{\max} = \frac{\pi}{2\lambda_2}$. The temperature connection to λ_2 is not known. However, like WCP, here also r_c plays same role: with progress in r_c , temperature effect enhances. Figure 1(b) imprints that, with rise in λ_2 the position of maximum gets left shifted and hence, plasma density advances. Like WCP, here too the effects of both λ_2 and r_c are explored. At $\lambda = 0$, both WCP and ECSCP modify to FHA-like systems.

In case of SCP, the ion experiences a spherically symmetric environment within a radius

R , commonly known as Wigner-Seitz radius. Beyond R , the effect of the potential vanishes. Hence the potential is expressed as,

$$V_3(r) = \begin{cases} = -\frac{Z}{r} + \frac{Z-N_e}{2R} \left[3 - \left(\frac{r}{R} \right)^2 \right], \\ = 0, & r > r_c = R. \end{cases} \quad (19)$$

With decrease in R , n_e increases and *vice versa*. T does not appear directly in this case. However, it is implicit that the change in R exerts the effect of T . At $r_c \rightarrow \infty$, Eq. (19) reduces to FHA. It is necessary to mention that, in SCP $Z \geq 2$ condition needs to be obeyed.

D. Scaling transformation

In case of plasma potentials, scaling concept has been implied previously in [7, 33, 36, 57]. This work employs two independent scaling ideas and attempts to derive a single equation connecting the original and scaled Hamiltonians. Thus, starting from an arbitrary set of Z and β , one can easily estimate a given desired property for a series of Z and β , connected by the scaling relation. To proceed further, one can write Eq. (3) as follows,

$$-\frac{\hbar^2}{2m} \frac{d^2}{dr^2} \psi_{n,\ell}(r) + V_c(Z; \beta; r) \psi_{n,\ell}(r) + V_0 \theta(r - r_c) \psi_{n,\ell}(r) = \mathcal{E}_{n,\ell} \psi_{n,\ell}(r), \quad (20)$$

$$\theta(r - r_c) = 0, \quad \text{at } r \leq r_c, \quad \theta(r - r_c) = 1, \quad \text{at } r > r_c.$$

Here $V_c(Z, \beta, r)$ is the potential that describes a H atom under the influence of plasma environment, $\theta(r - r_c)$ is Heaviside theta function and V_0 is taken to be an infinitely large positive constant. The use of atomic unit, $\hbar = m = 1$, transforms Eq. (20) as below,

$$-\frac{1}{2} \frac{d^2}{dr^2} \psi_{n,\ell}(r) + V_c(Z; \beta; r) \psi_{n,\ell}(r) + V_0 \theta(r - r_c) \psi_{n,\ell}(r) = \mathcal{E}_{n,\ell} \psi_{n,\ell}(r) \quad (21)$$

For H-isoelectronic series, it is interesting to probe the impact of Z as well as β , on the properties of a given system. Now analytical relations among $\langle T^n \rangle$, $\langle V^n \rangle$, $\langle TV \rangle$, $f_{ni}^{(k)}$, $\alpha_{ni}^{(k)}$ with Z and β will be established, by employing two independent, parallel scaling transformations.

- (i) In the first case, we apply a transformation ($r = Zr_1$). The Hamiltonian can then be modified in the following form,

$$H(Z; \beta; r_c; r) \rightarrow H\left(1; \frac{\beta}{Z}; Zr_c; r_1\right). \quad (22)$$

Thus, the Z -containing part of the potential becomes independent of it.

This substitution transforms the Hamiltonian in Eq. (20) in following form,

$$-\frac{1}{2}\nabla_1^2\psi_{n,\ell}(r_1) + V_c\left(1, \frac{\beta}{Z}, r_1\right)\psi_{n,\ell}(r_1) + Z^2V_0\theta(r_1 - Zr_c)\psi_{n,\ell}(r_1) \\ = Z^2\mathcal{E}_{n,\ell}\psi_{n,\ell}(r_1). \quad (23)$$

The eigenfunctions, eigenvalues of initial and modified Hamiltonians are connected as,

$$\mathcal{E}_{n,\ell}[1; Z; \beta; r_c] = Z^2\mathcal{E}_{n,\ell}\left[1; 1; \frac{\beta}{Z}; Zr_c\right], \\ \psi_{n,\ell}(1; Z; \beta; r_c; r) = \frac{1}{Z^{\frac{3}{2}}}\psi_{n,\ell}\left(1; 1; \frac{\beta}{Z}; Zr_c; r_1\right). \quad (24)$$

Then $\langle T^n \rangle, \langle V^n \rangle, \langle TV \rangle$ and Z are found to be related as,

$$\langle V^n \rangle[1; Z; \beta; r_c] = Z^{2n}\langle V^n \rangle\left[1; 1; \frac{\beta}{Z}; Zr_c\right], \quad \langle T^n \rangle[1; Z; \beta; r_c] = Z^{2n}\langle T^n \rangle\left[1; 1; \frac{\beta}{Z}; Zr_c\right] \\ \langle TV \rangle[1; Z; \beta; r_c] = Z^4\langle TV \rangle\left[1; 1; \frac{\beta}{Z}; Zr_c\right], \quad \langle VT \rangle[1; Z; \beta; r_c] = Z^4\langle VT \rangle\left[1; 1; \frac{\beta}{Z}; Zr_c\right] \quad (25)$$

The multipole OS now takes the form,

$$f_{ni}^{(k)}[1; Z; \beta; r_c] = \frac{f_{ni}^{(k)}\left[1; 1; \frac{\beta}{Z}; Zr_c\right]}{Z^{2(k-1)}}. \quad (26)$$

This equation suggests that, dipole ($k = 1$) OS is independent of this scaling transformation. However, quadrupole ($k = 2$), octupole ($k = 3$) and hexadecapole ($k = 4$) OSs depend on Z . Now, some simple mathematical manipulation provides the modified expression of $\alpha_i^{(k)}(\text{bound})$ as follows,

$$\alpha_i^{(k)}(\text{bound})[1; Z; \beta; r_c] = \frac{\alpha_i^{(k)}(\text{bound})\left[1; 1; \frac{\beta}{Z}; Zr_c\right]}{Z^{2k+2}}. \quad (27)$$

(ii) Another transformation ($r = \frac{r_2}{\beta}$), can be applied to alter the same Hamiltonian as,

$$H(Z; \beta; r_c; r) \rightarrow H\left(\frac{Z}{\beta}; 1; \beta r_c; r_2\right). \quad (28)$$

Now the potential is mapped such that, the β -containing part becomes free of it.

The substitution of $r = \frac{r_2}{\beta}$ transforms the Hamiltonian in Eq. (20) in the form,

$$-\frac{1}{2}\nabla^2\psi_{n,\ell}(r_2) + V_c\left(\frac{Z}{\beta}; 1; r_2\right)\psi_{n,\ell}(r_2) + \frac{1}{\beta^2}V_0\theta(r_2 - \beta r_c)\psi_{n,\ell}(r_2) \\ = \left(\frac{\mathcal{E}_{n,\ell}}{\beta^2}\right)\psi_{n,\ell}(r_2). \quad (29)$$

The eigenfunctions, eigenvalues of initial and modified Hamiltonians are related as,

$$\begin{aligned}\mathcal{E}_{n,\ell}[1; Z; \beta; r_c] &= \beta^2 \mathcal{E}_{n,\ell}\left[1; \frac{Z}{\beta}; 1; \beta r_c\right], \\ \psi_{n,\ell}(1; Z; \beta; r_c; r) &= \beta^{\frac{3}{2}} \psi_{n,\ell}\left(1; \frac{Z}{\beta}; 1; \beta r_c; r_2\right).\end{aligned}\tag{30}$$

Then $\langle T^n \rangle, \langle V^n \rangle, \langle TV \rangle$ and β are connected as,

$$\begin{aligned}\langle V^n \rangle [1; Z; \beta; r_c] &= \beta^{2n} \langle V^n \rangle \left[1; \frac{Z}{\beta}; 1; \beta r_c\right], & \langle T^n \rangle [1; Z; \beta; r_c] &= \beta^{2n} \langle T^2 \rangle \left[1; \frac{Z}{\beta}; 1; \beta r_c\right] \\ \langle TV \rangle [1; Z; \beta; r_c] &= \beta^4 \langle TV \rangle \left[1; \frac{Z}{\beta}; 1; \beta r_c\right], & \langle VT \rangle [1; Z; \beta; r_c] &= \beta^4 \langle VT \rangle \left[1; \frac{Z}{\beta}; 1; \beta r_c\right]\end{aligned}\tag{31}$$

Now, using Eq. (25) into Eq. (9), the multipole OS can have the generalized form,

$$f_{ni}^{(k)} [1; Z; \beta; r_c] = \left(\frac{f_{ni}^{(k)} \left[1; \frac{Z}{\beta}; 1; \beta r_c\right]}{\beta^{(2k-2)}} \right).\tag{32}$$

This implies that, dipole OS is invariant under this scaling transformation. However, higher order ($k > 1$) OS depend on β . Again some straightforward mathematical manipulation gives the modified expression of $\alpha_i^{(k)}(\text{bound})$ as,

$$\alpha_i^{(k)}(\text{bound}) [1; Z; \beta; r_c] = \left(\frac{\alpha_i^{(k)}(\text{bound}) \left[1; \frac{Z}{\beta}; 1; \beta r_c\right]}{\beta^{2(k+1)}} \right)\tag{33}$$

Thus we have successfully converted the initial Hamiltonian, Eq. (3) into two independent scaled Hamiltonians, *viz.*, Eqs. (23) and (29). Now, the connecting relations are,

$$\mathcal{E}_{n,\ell} [1; Z; \beta; r_c] = Z^2 \mathcal{E}_{n,\ell} \left[1; 1; \frac{\beta}{Z}; Z r_c\right] = \beta^2 \mathcal{E}_{n,\ell} \left[1; \frac{Z}{\beta}; 1; \beta r_c\right].\tag{34}$$

Some reorganization leads to the following,

$$\frac{\mathcal{E}_{n,\ell} \left[1; 1; \frac{\beta}{Z}; Z r_c\right]}{\mathcal{E}_{n,\ell} \left[1; \frac{Z}{\beta}; 1; \beta r_c\right]} = \left(\frac{\beta}{Z} \right)^2.\tag{35}$$

The expectation values then satisfy the following relations,

$$\langle V^n \rangle [1; Z; \beta; r_c] = Z^{2n} \langle V^n \rangle \left[1; 1; \frac{\beta}{Z}; Z r_c\right] = \beta^{2n} \langle V^n \rangle \left[1; \frac{Z}{\beta}; 1; \beta r_c\right].\tag{36}$$

A slight rearrangement of the above equation leads to,

$$\frac{\langle V^n \rangle \left[1; 1; \frac{\beta}{Z}; Z r_c\right]}{\langle V^n \rangle \left[1; \frac{Z}{\beta}; 1; \beta r_c\right]} = \left(\frac{\beta}{Z} \right)^{2n}.\tag{37}$$

In case of kinetic energy, one gets,

$$\langle T^n \rangle [1; Z; \beta; r_c] = Z^{2n} \langle T^n \rangle \left[1; 1; \frac{\beta}{Z}; Zr_c \right] = \beta^{2n} \langle T^n \rangle \left[1; \frac{Z}{\beta}; 1; \beta r_c \right]. \quad (38)$$

which, upon rearrangement, gives,

$$\frac{\langle T^n \rangle [1; 1; \frac{\beta}{Z}; Zr_c]}{\langle T^n \rangle [1; \frac{Z}{\beta}; 1; \beta r_c]} = \left(\frac{\beta}{Z} \right)^{2n}. \quad (39)$$

The multipole OS accordingly becomes,

$$f_{ni}^{(k)} [1; Z; \beta; r_c] = \frac{f_{ni}^{(k)} [1; 1; \frac{\beta}{Z}; Zr_c]}{Z^{2(k-1)}} = \frac{f_{ni}^{(k)} [1; \frac{Z}{\beta}; 1; \beta r_c]}{\beta^{2(k-1)}}. \quad (40)$$

which can be recast to yield,

$$\frac{f_{ni}^{(k)} [1; 1; \frac{\beta}{Z}; Zr_c]}{f_{ni}^{(k)} [1; \frac{Z}{\beta}; 1; \beta r_c]} = \left(\frac{Z}{\beta} \right)^{2(k-1)}. \quad (41)$$

Finally, the polarizabilities are connected as,

$$\alpha_i^{(k)}(\text{bound}) [1; Z; \beta; r_c] = \frac{\alpha_i^{(k)}(\text{bound}) [1; 1; \frac{\beta}{Z}; Zr_c]}{Z^{2(k+1)}} = \frac{\alpha_i^{(k)}(\text{bound}) [1; \frac{Z}{\beta}; 1; \beta r_c]}{\beta^{2(k+1)}}. \quad (42)$$

This can be written in the following form,

$$\frac{\alpha_i^{(k)}(\text{bound}) [1; 1; \frac{\beta}{Z}; Zr_c]}{\alpha_i^{(k)}(\text{bound}) [1; \frac{Z}{\beta}; 1; \beta r_c]} = \left(\frac{Z}{\beta} \right)^{2(k+1)}. \quad (43)$$

The foregoing discussion thus shows that, a connection formula, as below, can be derived among three Hamiltonians, corresponding to the SE in Eqs. (3), (23) and (29), *viz.*,

$$H \left(1; 1; \frac{\beta}{Z}; Zr_c; r_1 \right) \leftrightarrow H(1; Z; \beta; r_c; r) \leftrightarrow H \left(1; \frac{Z}{\beta}; 1; \beta r_c; r_2 \right) \quad (44)$$

The above equation signifies that, performing the calculation at a particular (Z, β) pair, one can evaluate the properties of other pair of (Z, β) (connected by scaling), without solving the SE. These are derived for any two-parameter potentials. These relations are applicable in all the three potentials used for the plasma characteristics in Sec. II.C. In WCP, ECSCP and SCP, β becomes $\lambda_1, \lambda_2, \sigma = \left(\frac{Z - Ne}{2R^3} \right)^{\frac{1}{4}}$ respectively. Some representative numerical results $(\mathcal{E}_{n,\ell}, f_{ns \rightarrow 2p}^{(1)}, \alpha_{ns}^{(1)})$ for these three Hamiltonians (connecting WCP, ECSCP, SCP) have been provided in Table V of Appendix B.

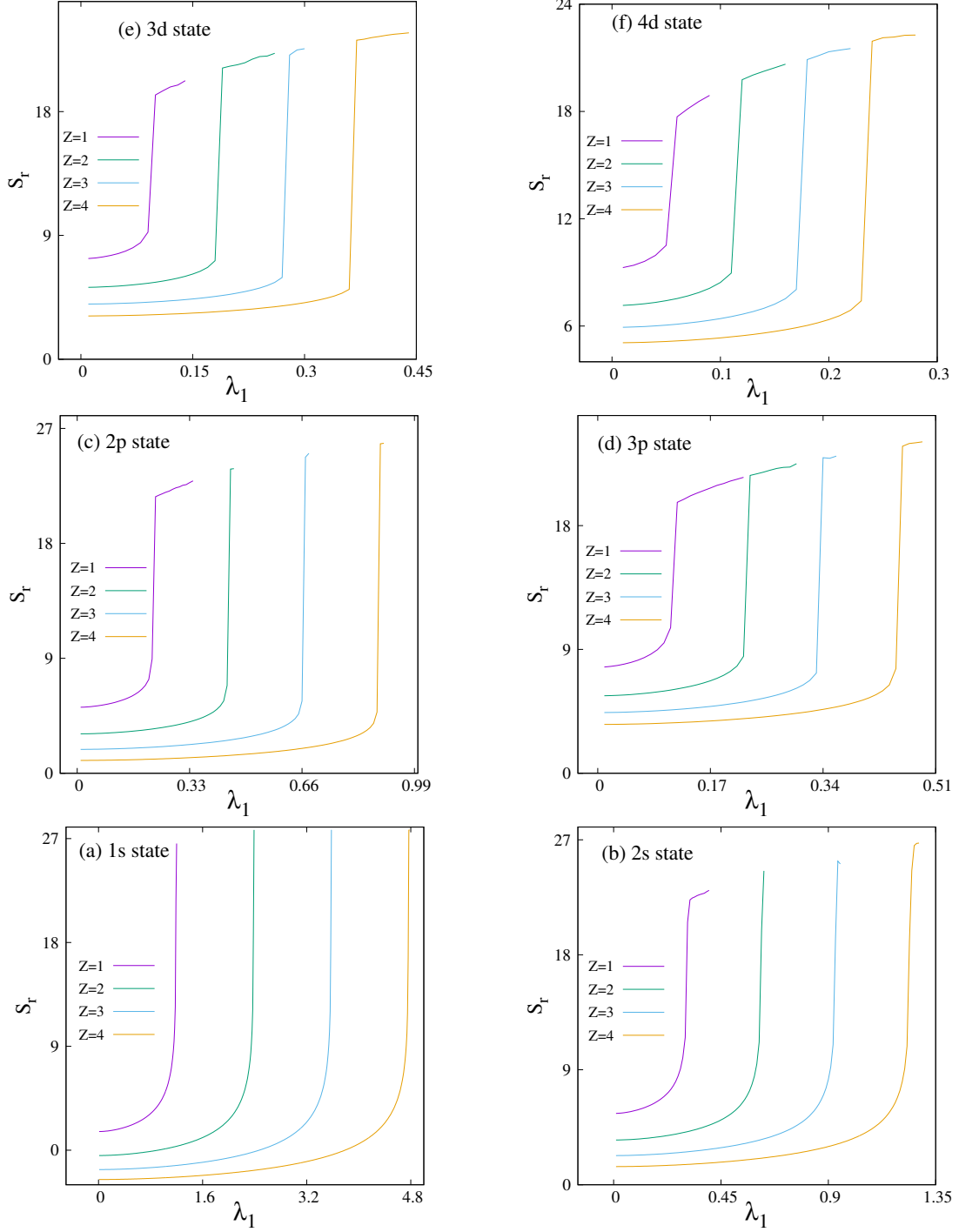


FIG. 2: Plot of S_c as function of λ_1 in WCP for (a) 1s (b) 2s (c) 2p (d) 3p (e) 3d, and (f) 4d states at four selected values of Z , namely, 1, 2, 3, 4. See text for details.

III. RESULT AND DISCUSSION

In this section at first, we will discuss the critical screening constant in WCP and ECSCP. Then, the usefulness and efficacy of VT will be verified for WCP, ECSCP and SCP succes-

sively. Next, we report the multipole OS and polarizabilities for all these three potentials. Pilot calculations are done for $1s$ and $2s$ states choosing $Z = 2$. Of course, employing the scaling relations of Eqs. (24-27), one can easily extract the result for other Z values. For ease of convenience, we have adopted the following notation. Use of λ in the text implies *both* λ_1, λ_2 , while explicit use of λ_1 or λ_2 refers to WCP and ECSCP only.

A. Critical screening constant in WCP and ECSCP

In WCP and ECSCP (at $r_c \rightarrow \infty$), the number of bound states reduces with rise in screening parameter λ . Several attempts were made to estimate the characteristic value of λ at which a particular state vanishes. Accurate numerical results are available up to $6h$ states of H-atom in WCP [37, 66] and ECSCP [40, 51, 66]. Further, in [36], the relation between this critical constant $\lambda_{n,\ell}^{(c)}(Z)$ and Z was derived for ground state in WCP. These values are determined by applying the sign-change argument in energy. In stead of that, here, we have applied a simple density-based technique to ascertain these points in WCP and ECSCP. For that purpose, Shannon entropy ($S_r = - \int \rho(r) \ln \rho(r) r^2 dr$) [67] has been employed. Based on this study, a uniform relation between these two quantities ($\lambda_{n,\ell}^{(c)}(Z)$ and Z) is offered. This may be applied to an arbitrary state. Furthermore, a similar relation is also obtained by employing the scaling concept and some empirical idea (see below).

The calculated S_r , as a function of λ_1 for first two states of each $\ell = 0 - 2$ are displayed in Fig. 2. Panels (a)-(f) represent $1s, 2s, 2p, 3p, 3d, 4d$ states respectively. In each of these panels one can see equi-spaced curves corresponding to $Z = 1 - 4$. At a fixed Z , in each of these states there occurs a sudden jump in S_r at a characteristic λ_1 . Therefore, S_r can indicate the critical point, at which a particular state vanishes. Further, at a certain Z , S_r increases with λ_1 . It means that with decrease in D confinement effect weakens. Conversely, with rise in T this effect predominates. Analogous plots are supplied in Fig. 3(a)-3(f) for ECSCP, involving same 6 states of Fig. 2. The qualitative behavior of S_r in WCP and ECSCP remains quite similar. In each state, a stiff increase in S_r occurs at certain λ_2 value. Interestingly, with rise in Z , this S_r vs λ_2 curve gets right shifted. Further, these curves are placed equidistant from each other. From the above, it is clear that, S_r can be used in determining critical screening constant in a given potential. Note that, in both potentials, for a given state, the ratio of screening constant and Z is a constant, because,

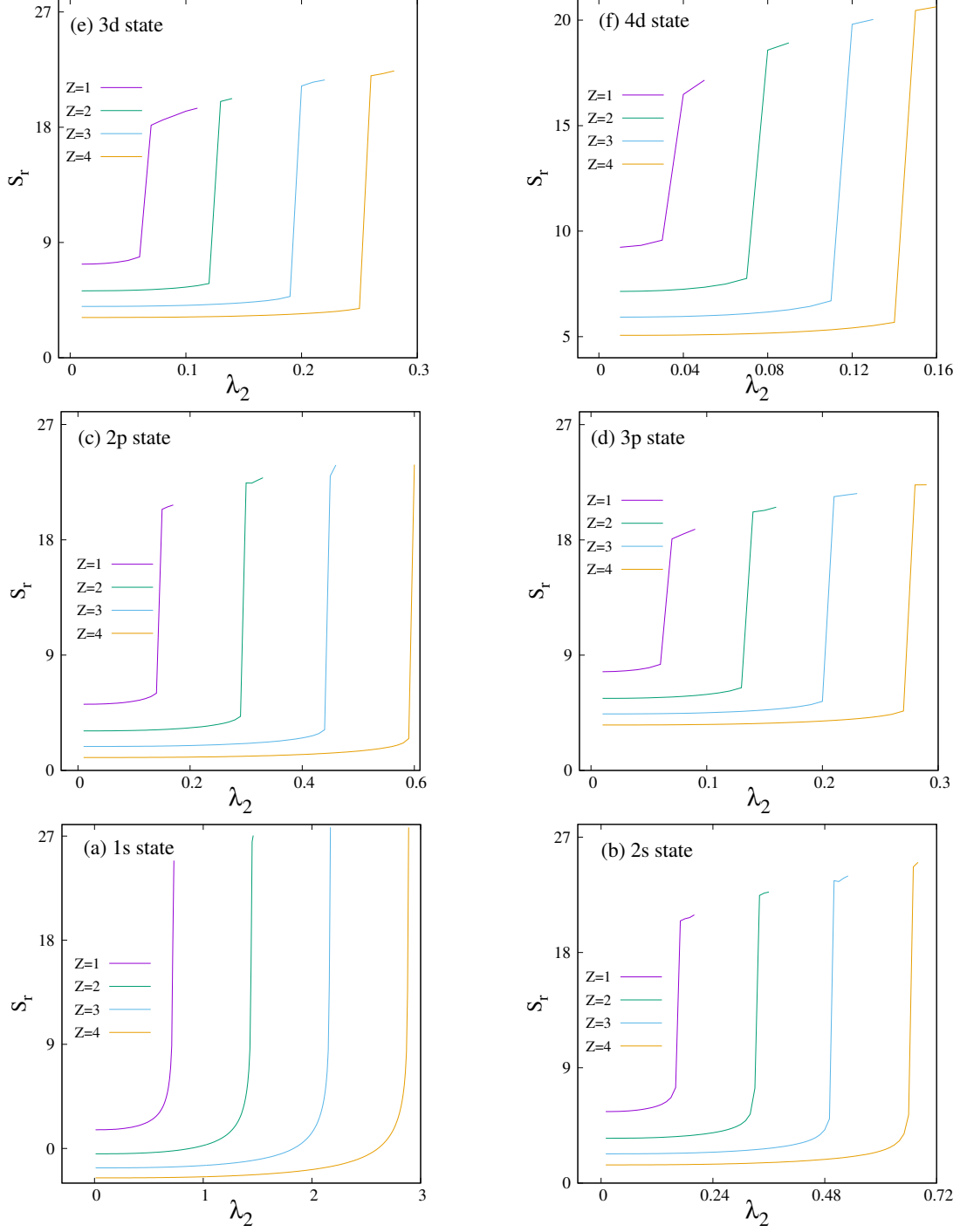


FIG. 3: Plot of S_r as function of λ_2 in ECSCP for (a) 1s (b) 2s (c) 2p (d) 3p (e) 3d, and (f) 4d states at four selected values of Z , namely, 1, 2, 3, 4. See text for details.

the four curves remain evenly separated. Depending upon these outcomes one can derive an empirical relation between $\lambda_{n,\ell}$ and Z .

TABLE I: $\lambda_{n,\ell}^{(c)}$ for H-like ion for $1s, 2s, 2p, 3p, 3d, 4d$ states in WCP, ECSCP. See text for details.

WCP				ECSCP			
Z	State	$\lambda_{n,\ell}^{(c)}$	$\mathcal{E}_{n,\ell}$	Z	State	$\lambda_{n,\ell}^{(c)}$	$\mathcal{E}_{n,\ell}$
1	1s	1.1856 ^{‡,†}	−0.00000656	1	1s	0.7196 [§]	−0.00000531
2		2.3712	−0.00002650	2	1s	1.4384	−0.00002124
3		3.5573	−0.00005964	3	1s	2.1576	−0.00004779
4		4.7410	−0.00010265	4	1s	2.8756	−0.00008496
1	2s	0.3063 [‡]	−0.00000995	1	2s	0.1664 [§]	−0.00000552
2		0.6124	−0.00003960	2	2s	0.3328	−0.00002206
3		0.9195	−0.00008970	3	2s	0.4992	−0.00004965
4		1.2254	−0.00015925	4	2s	0.6656	−0.00008826
1	2p	0.2206 [‡]	−0.00000723	1	2p	0.1482 [§]	−0.00000234
2		0.4404	−0.00002860	2	2p	0.2964	−0.00000937
3		0.6606	−0.00006341	3	2p	0.4446	−0.00002109
4		0.8821	−0.00011341	4	2p	0.5928	−0.00003749
1	3p	0.1126 [‡]	−0.00000701	1	3p	0.0687 [§]	−0.00000488
2		0.2254	−0.00002854	2	3p	0.1374	−0.00001950
3		0.3381	−0.00006371	3	3p	0.2061	−0.00004388
4		0.4504	−0.00011208	4	3p	0.2748	−0.00007801
1	3d	0.0914 [‡]	−0.00000878	1	3d	0.0635 [§]	−0.00001937
2		0.1826	−0.00003614	2	3d	0.1271	−0.00007787
3		0.2739	−0.00008030	3	3d	0.1907	−0.00017251
4		0.3653	−0.00012718	4	3d	0.2542	−0.00031150
1	4d	0.0581 [‡]	−0.00000974	1	4d	0.0374 [§]	−0.00000260
2		0.1161	−0.00003951	2	4d	0.0748	−0.00001041
3		0.1741	−0.00008364	3	4d	0.1122	−0.00002342
4		0.2321	−0.00016672	4	4d	0.1496	−0.00004164

[†]Literature result of $\lambda_{1,0}^{(c)}$ [7]: 1.190612421.

[‡]Literature results of $\lambda_{n,\ell}^{(c)}$ [51, 66]: (a) $\lambda_{1s}^{(c)} = 1.190610$ (b) $\lambda_{2s}^{(c)} = 0.310199$ (c) $\lambda_{2p}^{(c)} = 0.220216$ (d) $\lambda_{3p}^{(c)} = 0.112710$ (e) $\lambda_{3d}^{(c)} = 0.091345$ (f) $\lambda_{4d}^{(c)} = 0.058105$.

[§]Literature results of $\lambda_{n,\ell}^{(c)}$ [40, 51, 66]: (a) $\lambda_{1s}^{(c)} = 0.720524$ (b) $\lambda_{2s}^{(c)} = 0.166617$ (c) $\lambda_{2p}^{(c)} = 0.148205$ (d) $\lambda_{3p}^{(c)} = 0.068712$ (e) $\lambda_{3d}^{(c)} = 0.063581$ (f) $\lambda_{4d}^{(c)} = 0.037405$.

Both in WCP and ECSCP, the Hamiltonian in *free condition* is scaled as,

$$H(Z; \lambda) \rightarrow H\left(1; \frac{\lambda}{Z}\right). \quad (45)$$

Similarly energy in a definite (n, ℓ) state is scaled as,

$$\mathcal{E}_{n,\ell}(Z; \lambda) = Z^2 \mathcal{E}_{n,\ell}\left(1; \frac{\lambda}{Z}\right) \quad (46)$$

Therefore, one can easily write the following relations for both WCP and ECSCP cases,

$$\begin{aligned}\frac{\lambda_{n,\ell}^{(c)}}{Z} &\approx \lambda_{n,\ell}^{(c)}(Z=1), \\ \lambda_{n,\ell}^{(c)}(Z) &\approx Z \lambda_{n,\ell}^{(c)}(Z=1).\end{aligned}\tag{47}$$

This relation in Eq. (47) is in excellent agreement with those achieved by computing S_r in WCP and ECSCP. Representative numerical results are provided in Table I for $Z = 1 - 4$ involving the same six states of Figs. 1 and 2, in WCP and ECSCP. These critical parameters are compared with available reference results (for $Z = 1$). which shows very good matching in both WCP [51, 66] and ECSCP [40, 51, 66]. However, to the best of our knowledge, no such data are reported till date for $Z > 1$. The critical points from sign change argument also complement the outcomes achieved by employing the information entropy concept. This shows that S_r may act as an efficient indicator for finding critical points and may be utilized in future. As expected, the tabular results strongly recommend the proposition of Eq. (47) in both WCP and ECSCP. For the sake of completeness, $\lambda_{n,\ell}^{(c)}$ are computed for all the remaining states corresponding to $\ell = 5$ ($3s, 4s, 4p, 4f, 5s, 5p, 5d, 5f, 5g$). They are reported in Table VI of Appendix C, along with the appropriate references.

B. Virial-like Theorem

As mentioned in Sec. II.A, the conventional VT is not satisfied in confined condition. Recently [59], a virial-like expression is derived and successfully applied in H-atom trapped in various confined environment [59]. It is found that, at the end, the perturbing potential does not appear in the final expression. In this subsection, we are probing this theorem in the context of WCP, ECSCP and SCP successively.

In WCP, the necessary expectation values will take the form,

$$\begin{aligned}\langle TV \rangle_{n,\ell} &= \left\langle T \left(-\frac{Z}{r} e^{(-\lambda_1 r)} \right) \right\rangle_{n,\ell}, & \langle VT \rangle_{n,\ell} &= \left\langle \left(-\frac{Z}{r} e^{(-\lambda_1 r)} \right) T \right\rangle_{n,\ell}, \\ \langle V^2 \rangle_{n,\ell} &= \left\langle \frac{Z^2}{r^2} e^{(-2\lambda_1 r)} \right\rangle_{n,\ell}, & \langle V \rangle_{n,\ell} &= \left\langle -\frac{Z}{r} e^{(-\lambda_1 r)} \right\rangle_{n,\ell}.\end{aligned}\tag{48}$$

TABLE II: $\mathcal{E}_{n,\ell}, (\Delta V_{n,\ell})^2, (\Delta T_{n,\ell})^2, \langle T \rangle_{n,\ell} \langle V \rangle_{n,\ell} - \langle TV \rangle_{n,\ell}, \langle T \rangle_{n,\ell} \langle V \rangle_{n,\ell} - \langle VT \rangle_{n,\ell}$ of $1s, 2s$ states in WCP, ECSCP and SCP, choosing $Z = 2$, at six different sets of $(\lambda_1, r_c), (\lambda_2, r_c)$ and r_c respectively.

WCP							
State	Quantity	$\lambda_1 = 0.1$	$\lambda_1 = 0.1$	$\lambda_1 = 0.5$	$\lambda_1 = 1$	$\lambda_1 = 1.5$	$\lambda_1 = 0.45$
		$r_c = 0.1$	$r_c = 0.5$	$r_c = 0.5$	$r_c = 1$	$r_c = 5$	$r_c = \infty$
1s	$\mathcal{E}_{1,0}$	444.47894213	9.69364280	10.43995746	1.13262338	-0.22737500	-1.23411551
	$(\Delta V_{1,0})^2$	1285.99378348	71.83641411	71.53062216	26.32910366	8.20218577	15.00733998
	$(\Delta T_{1,0})^2$	1285.99378348	71.83641411	71.53062216	26.32910366	8.20218577	15.00733998
	$\langle T \rangle_{1,0} \langle V \rangle_{1,0} - \langle TV \rangle_{1,0}$	1285.99378355	71.83641411	71.53062216	26.32910366	8.20218577	15.00733998
	$\langle T \rangle_{1,0} \langle V \rangle_{1,0} - \langle VT \rangle_{1,0}$	1285.99378355	71.83641411	71.53062216	26.32910366	8.20218577	15.00733998
2s	$\mathcal{E}_{2,0}$	1911.60619014	66.47853464	67.22135372	14.89326554	0.38477218	-0.02806813
	$(\Delta V_{2,0})^2$	3787.39749470	180.91460373	180.32580299	53.43300740	3.14499616	1.08218497
	$(\Delta T_{2,0})^2$	3787.39749470	180.91460373	180.32580299	53.43300740	3.14499616	1.08218497
	$\langle T \rangle_{2,0} \langle V \rangle_{2,0} - \langle TV \rangle_{2,0}$	3787.39749467	180.91460373	180.32580300	53.43300740	3.14499616	1.08218497
	$\langle T \rangle_{2,0} \langle V \rangle_{2,0} - \langle VT \rangle_{2,0}$	3787.39749467	180.91460373	180.32580300	53.43300740	3.14499616	1.08218497
ECSCP							
State	Quantity	$\lambda_2 = 0.1$	$\lambda_2 = 0.1$	$\lambda_2 = 0.5$	$\lambda_2 = 1$	$\lambda_2 = 1.5$	$\lambda_2 = 0.25$
		$r_c = 0.1$	$r_c = 0.5$	$r_c = 0.5$	$r_c = 1$	$r_c = 5$	$r_c = \infty$
1s	$\mathcal{E}_{1,0}$	444.47943354	9.69592190	10.49107011	1.39032540	0.07291645	-1.50671442
	$(\Delta V_{1,0})^2$	1286.00324892	71.84954944	71.80723304	27.20420371	4.95684246	15.91293469
	$(\Delta T_{1,0})^2$	1286.00324892	71.84954944	71.80723304	27.20420371	4.95684246	15.91293469
	$\langle T \rangle_{1,0} \langle V \rangle_{1,0} - \langle TV \rangle_{1,0}$	1286.00324885	71.84954944	71.80723304	27.20420371	4.95684246	15.91293469
	$\langle T \rangle_{1,0} \langle V \rangle_{1,0} - \langle VT \rangle_{1,0}$	1286.00324885	71.84954944	71.80723304	27.20420371	4.95684246	15.91293469
2s	$\mathcal{E}_{2,0}$	1911.60668730	66.48097112	67.27483408	15.15621209	0.49330671	-0.07314818
	$(\Delta V_{2,0})^2$	3787.42042508	180.93992940	180.85424331	54.56130508	4.89088914	2.26239187
	$(\Delta T_{2,0})^2$	3787.42042508	180.93992940	180.85424331	54.56130508	4.89088914	2.26239187
	$\langle T \rangle_{2,0} \langle V \rangle_{2,0} - \langle TV \rangle_{2,0}$	3787.42042492	180.93992940	180.85424331	54.56130508	4.89088914	2.26239187
	$\langle T \rangle_{2,0} \langle V \rangle_{2,0} - \langle VT \rangle_{2,0}$	3787.42042492	180.93992940	180.85424331	54.56130508	4.89088914	2.26239187
SCP							
State	Quantity	$r_c = 0.1$	$r_c = 0.5$	$r_c = 1$	$r_c = 2$	$r_c = 5$	$r_c = 10$
		$r_c = 0.1$	$r_c = 0.5$	$r_c = 1$	$r_c = 2$	$r_c = 5$	$r_c = 10$
1s	$\mathcal{E}_{1,0}$	471.50566905	14.98747298	2.27917566	-0.50537037	-1.40602867	-1.70075051
	$(\Delta V_{1,0})^2$	1207.82025521	67.49838821	26.33780873	16.31778893	15.91807847	15.98870703
	$(\Delta T_{1,0})^2$	1207.82025521	67.49838821	26.33780873	16.31778893	15.91807847	15.98870703
	$\langle T \rangle_{1,0} \langle V \rangle_{1,0} - \langle TV \rangle_{1,0}$	1207.82025512	67.49838821	26.33780873	16.31778893	15.91807847	15.98870703
	$\langle T \rangle_{1,0} \langle V \rangle_{1,0} - \langle VT \rangle_{1,0}$	1207.82025512	67.49838821	26.33780873	16.31778893	15.91807847	15.98870703
2s	$\mathcal{E}_{2,0}$	1938.19369550	71.63098684	15.97749590	3.00469070	0.09030651	-0.21064190
	$(\Delta V_{2,0})^2$	3589.04237047	172.06135205	53.23498447	18.29571481	3.69613370	2.88000313
	$(\Delta T_{2,0})^2$	3589.04237047	172.06135205	53.23498447	18.29571481	3.69613370	2.88000313
	$\langle T \rangle_{2,0} \langle V \rangle_{2,0} - \langle TV \rangle_{2,0}$	3589.04237064	172.06135205	53.23498447	18.29571481	3.69613370	2.88000313
	$\langle T \rangle_{2,0} \langle V \rangle_{2,0} - \langle VT \rangle_{2,0}$	3589.04237064	172.06135205	53.23498447	18.29571481	3.69613370	2.88000313

Now, applying the expression of Eq. (48) in Eq. (5) we obtain,

$$\begin{aligned}
\langle T^2 \rangle_{n,\ell} - \langle T \rangle_{n,\ell}^2 &= (\Delta T_{n,\ell})^2 = \langle V^2 \rangle_{n,\ell} - \langle V \rangle_{n,\ell}^2 = (\Delta V_{n,\ell})^2 \\
&= \left\langle \frac{Z^2}{r^2} e^{(-2\lambda_1 r)} \right\rangle_{n,\ell} - \left\langle \frac{Z}{r} e^{(-\lambda_1 r)} \right\rangle_{n,\ell}^2 \\
&= \langle T \rangle_{n,\ell} \left\langle -\frac{Z}{r} e^{(-\lambda_1 r)} \right\rangle_{n,\ell} - \left\langle T \left(-\frac{Z}{r} e^{(-\lambda_1 r)} \right) \right\rangle_{n,\ell}.
\end{aligned} \tag{49}$$

The relevant expectation values in ECSCP are expressed as,

$$\begin{aligned}
\langle TV \rangle_{n,\ell} &= \left\langle T \left(-\frac{Z}{r} e^{(-\lambda_2 r)} \cos \lambda_2 r \right) \right\rangle_{n,\ell}, \quad \langle VT \rangle_{n,\ell} = \left\langle \left(-\frac{Z}{r} e^{(-\lambda_1 r)} \cos \lambda_2 r \right) T \right\rangle_{n,\ell}, \\
\langle V^2 \rangle_{n,\ell} &= \left\langle \frac{Z^2}{r^2} e^{(-2\lambda_2 r)} \cos^2 \lambda_2 r \right\rangle_{n,\ell}, \quad \langle V \rangle_{n,\ell} = \left\langle -\frac{Z}{r} e^{(-\lambda_2 r)} \cos \lambda_2 r \right\rangle_{n,\ell}.
\end{aligned} \tag{50}$$

Now, substituting the results of Eq. (50) in Eq. (5) we achieve,

$$\begin{aligned}
\langle T^2 \rangle_{n,\ell} - \langle T \rangle_{n,\ell}^2 &= (\Delta T_{n,\ell})^2 = \langle V^2 \rangle_{n,\ell} - \langle V \rangle_{n,\ell}^2 = (\Delta V_{n,\ell})^2 \\
&= \left\langle \frac{Z^2}{r^2} e^{(-2\lambda_2 r)} \cos^2 \lambda_2 r \right\rangle_{n,\ell} - \left\langle \frac{Z}{r} e^{(-\lambda_2 r)} \cos \lambda_2 r \right\rangle_{n,\ell}^2 \\
&= \langle T \rangle_{n,\ell} \left\langle -\frac{Z}{r} e^{(-\lambda_2 r)} \cos \lambda_2 r \right\rangle_{n,\ell} - \left\langle T \left(-\frac{Z}{r} e^{(-\lambda_2 r)} \right) \cos \lambda_2 r \right\rangle_{n,\ell}.
\end{aligned} \tag{51}$$

In SCP, the respective expectation values are manifested as,

$$\begin{aligned}
\langle TV \rangle_{n,\ell} &= \left\langle T \left[-\frac{Z}{r} + \frac{(Z - N_e)}{R} \left(3 - \left(\frac{r}{R} \right)^2 \right) \right] \right\rangle_{n,\ell}, \\
\langle VT \rangle_{n,\ell} &= \left\langle \left[-\frac{Z}{r} + \frac{(Z - N_e)}{R} \left(3 - \left(\frac{r}{R} \right)^2 \right) \right] T \right\rangle_{n,\ell}, \\
\langle V^2 \rangle_{n,\ell} &= \left\langle \left[-\frac{Z}{r} + \frac{(Z - N_e)}{R} \left(3 - \left(\frac{r}{R} \right)^2 \right) \right]^2 \right\rangle_{n,\ell}, \\
\langle V \rangle_{n,\ell} &= \left\langle \left[-\frac{Z}{r} + \frac{(Z - N_e)}{R} \left(3 - \left(\frac{r}{R} \right)^2 \right) \right] \right\rangle_{n,\ell}.
\end{aligned} \tag{52}$$

Finally, engaging the outcome of Eq. (52) in Eq. (5) becomes,

$$\begin{aligned}
\langle T^2 \rangle_{n,\ell} - \langle T \rangle_{n,\ell}^2 &= (\Delta T_{n,\ell})^2 = \langle V^2 \rangle_{n,\ell} - \langle V \rangle_{n,\ell}^2 = (\Delta V_{n,\ell})^2 \\
&= \left\langle \left[-\frac{Z}{r} + \frac{(Z - N_e)}{R} \left(3 - \left(\frac{r}{R} \right)^2 \right) \right]^2 \right\rangle_{n,\ell} - \left\langle \left[-\frac{Z}{r} + \frac{(Z - N_e)}{R} \left(3 - \left(\frac{r}{R} \right)^2 \right) \right] \right\rangle_{n,\ell}^2 \\
&= \langle T \rangle_{n,\ell} \left\langle \left[-\frac{Z}{r} + \frac{(Z - N_e)}{R} \left(3 - \left(\frac{r}{R} \right)^2 \right) \right] \right\rangle_{n,\ell} - \left\langle T \left[-\frac{Z}{r} + \frac{(Z - N_e)}{R} \left(3 - \left(\frac{r}{R} \right)^2 \right) \right] \right\rangle_{n,\ell}.
\end{aligned} \tag{53}$$

TABLE III: $f^{(1)}$ values for WCP, ECSCP (in free and confined conditions) and SCP involving $ns \rightarrow 2p$, $ns \rightarrow 3p$ ($n = 1, 2$) transitions. See text for details.

Transition	Confined WCP						Free WCP	
	λ_1	$r_c = 0.1$	$r_c = 0.5$	$r_c = 1$	$r_c = 2$	$r_c = 5$	λ_1	$r_c = \infty$
$1s \rightarrow 2p$	0.1	0.97072714	0.98455633	0.99105667	0.92744965	0.48674542	0.1	0.40181907
	0.5	0.97072657	0.98450970	0.99101296	0.93172951	0.42593118	0.2	0.36301391
	1	0.97072481	0.98437662	0.99088526	0.94270974	0.42487213	0.3	0.29859664
	2.2	0.97071618	0.98380464	0.99014361	0.97196847	0.84116523	0.4	0.19333749
$1s \rightarrow 3p$	0.1	0.02145207	0.00772756	0.00000194	0.04896547	0.30906124	0.01	0.07892729
	0.5	0.02145255	0.00776480	0.00000008	0.04498399	0.32619988	0.05	0.07536052
	1	0.02145402	0.00787227	0.00002302	0.03498548	0.07783255	0.1	0.06581437
	2.2	0.02146127	0.00834459	0.00047966	0.00951569	0.26193927	0.2	0.02982086
$2s \rightarrow 2p$	0.1	-0.59617944	-0.60825425	-0.61188356	-0.54000701	-0.06993817	0.1	0.01961263
	0.4	-0.59617891	-0.60820263	-0.61167657	-0.54121728	0.00417437	0.2	0.07522974
	0.5	-0.59617859	-0.60817302	-0.61156439	-0.54200502	0.03181610	0.3	0.17737202
	1	-0.59617598	-0.60794575	-0.61078004	-0.54873672	0.07905123	0.4	0.37896055
$2s \rightarrow 3p$	0.1	1.53239528	1.56032134	1.57779183	1.51296821	0.96212776	0.01	0.43399889
	0.4	1.53239452	1.56024714	1.57830084	1.51388585	0.90876197	0.05	0.41594460
	0.5	1.53239406	1.56020449	1.57797157	1.51453142	0.88783614	0.1	0.36639711
	1	1.53239034	1.55987605	1.57652076	1.52043617	0.85542392	0.2	0.17105455
Transition	Confined ECSCP						Free ECSCP	
	λ_2	$r_c = 0.1$	$r_c = 0.5$	$r_c = 1$	$r_c = 2$	$r_c = 5$	λ_2	$r_c = \infty$
$1s \rightarrow 2p$	0.1	0.97072717	0.98455833	0.99105855	0.92726266	0.49020012	0.05	0.41541265
	0.5	0.97072715	0.98455130	0.99103661	0.92859601	0.39261746	0.1	0.41059123
	1	0.97072703	0.98450670	0.99091497	0.93723099	0.38873757	0.2	0.37680897
	1.4	0.97072679	0.98442680	0.99070952	0.95086935	0.72484192	0.25	0.33815629
$1s \rightarrow 3p$	0.1	0.02145205	0.00772596	0.00000215	0.04914057	0.25938284	0.01	0.07908337
	0.5	0.02145206	0.00773097	0.00000111	0.04772537	0.32705934	0.05	0.07727923
	1	0.02145216	0.00776310	0.00000195	0.03909999	0.33012451	0.1	0.06672974
	1.4	0.02145234	0.00782141	0.00003015	0.02603893	0.12347883	0.12	0.05778373
$2s \rightarrow 2p$	0.05	-0.59617948	-0.60825787	-0.61189909	-0.53993757	-0.07746440	0.05	0.00099592
	0.1	-0.59617948	-0.60825776	-0.61189792	-0.53993008	-0.07524706	0.1	0.00719122
	0.5	-0.59617945	-0.60824322	-0.61176097	-0.53953695	0.07707677	0.2	0.05235875
	1	-0.59617924	-0.60815247	-0.61102508	-0.54115043	0.16873325	0.25	0.10793827
$2s \rightarrow 3p$	0.05	1.53239533	1.56032654	1.57832534	1.51292362	0.96729789	0.01	0.43478301
	0.1	1.53239533	1.56032638	1.57832365	1.51291209	0.96572414	0.05	0.42653220
	0.5	1.53239529	1.56030638	1.57812514	1.51213836	0.84864260	0.1	0.37668282
	1	1.53239501	1.56018160	1.57705831	1.51229530	0.76798664	0.12	0.33241753
SCP								
Transition	$r_c = 0.1$	$r_c = 0.2$	$r_c = 0.5$	$r_c = 1$	$r_c = 2$	$r_c = 2.5$	$r_c = 5$	$r_c = 10$
$1s \rightarrow 2p$	0.97051035	0.97420550	0.98379490	0.99067302	0.92958863	0.84910611	0.46356524	0.40514594
$1s \rightarrow 3p$	0.02161960	0.01795866	0.00826516	0.00002030	0.04648691	0.10750364	0.27699337	0.10047172
$2s \rightarrow 2p$	-0.59580794	-0.59894650	-0.60667433	-0.60974041	-0.53810301	-0.45106011	-0.03771967	0.01415902
$2s \rightarrow 3p$	1.53188858	1.53916195	1.55815448	1.57522845	1.51008687	1.41740733	0.93835324	0.51932973

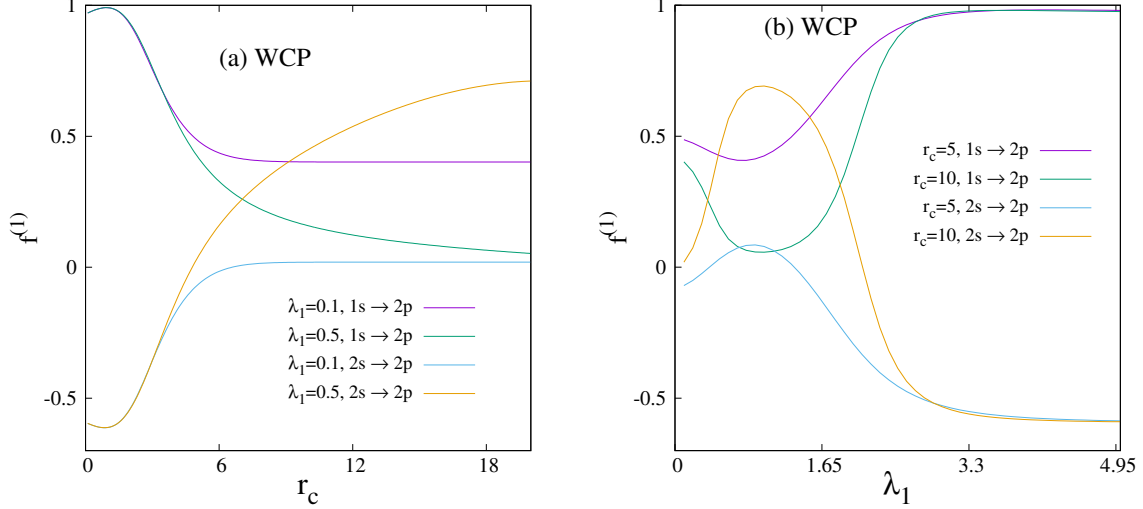


FIG. 4: $f_{ns \rightarrow 2p}^{(1)}(n = 1, 2)$ for WCP. Panel (a) gives r_c variation at two selected λ_1 (0.1, 0.5), while panel (b) shows λ_1 variation at two different r_c (5, 10). See text for details.

The upper segment of Table II represents results for WCP in $1s$ and $2s$ states at six different sets of $\{\lambda_1, r_c\}$ values, namely (0.1, 0.1), (0.1, 0.5), (0.5, 0.5), (1, 1), (1.5, 5), (0.45, ∞). In all these cases, Eq. (5) of Sec. II.A is corroborated. More importantly, in a given state, at a fixed r_c , energy increases with λ_1 . Similarly, at a certain λ_1 , it declines with rise in r_c . In the middle portion, the corresponding outcomes are tabulated for ECSCP at six chosen (λ_2, r_c) values, *viz.*, (0.1, 0.1), (0.1, 0.5), (0.5, 0.5), (1, 1), (1.5, 5), (0.25, ∞). Again, these data support the conclusion drawn from Eq. (5). Like the WCP, here also energy enhances with λ_2 at fixed r_c , and diminishes with r_c at a specific λ_2 . In the bottom part, numerical data about the validity of VT in the context of SCP are presented. Like the earlier two cases, this also satisfies Eq. (5). It may be mentioned that, a few attempts were made before to establish such a theorem in confined condition (that includes plasma environment), by means of Hellmann-Feynman theorem and conventional VT [36, 68]. There, the mathematical form of the expression changes from system to system; the present form, on the other hand, provides a uniform mathematical expression *irrespective of the system of interest*.

C. Multipole oscillator strengths and polarizabilities

In the following discussion, $Z = 2$ is chosen; that means, in SCP, β only depends on r_c . Hence, in SCP, the results are provided with respect to variation of r_c only. It may be recalled from Sec. II.C that in SCP, Z is required to be greater than 1. That is why, we

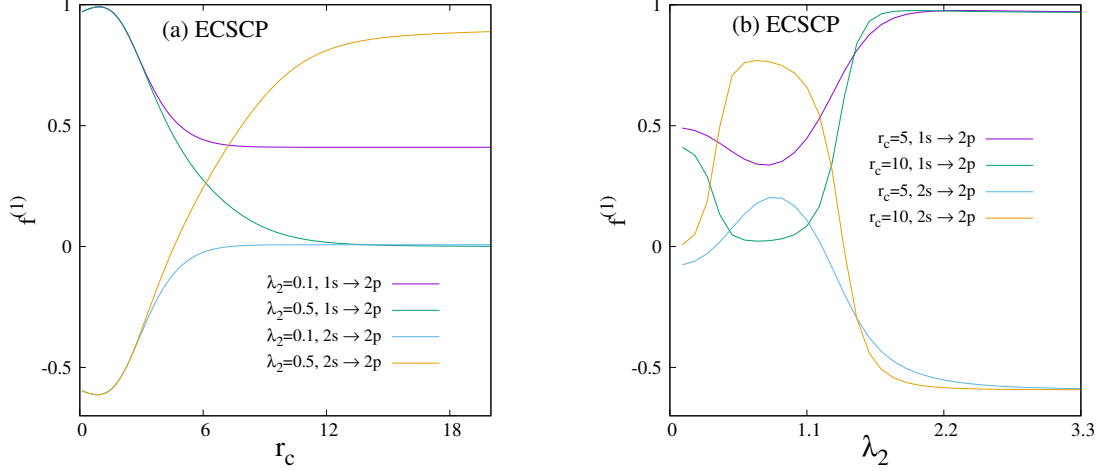


FIG. 5: $f_{ns \rightarrow 2p}^{(1)} (n = 1, 2)$ for ECSCP. Panel (a) gives r_c variation at two selected λ_2 (0.1, 0.5), while panel (b) shows λ_2 variation at two different r_c (5, 10). See text for details.

have selected $Z = 2$ in stead of 1, for all three environments. Note that, results for $Z = 1$ in *free* WCP and ECSCP were also calculated. They are found to be in consonance with available literature (see, e.g., [7, 9], and references therein). In this work, the primary focus, however, lies on *confined* plasma systems. The multipole OS sum rule given in Eq. (16) were estimated in both $1s$ and $2s$ states, involving all four k ($k = 1, 2, 3, 4$). In both *free* and *confined* conditions, this equation was obeyed. Further, this sum rule remains invariant under scaling transformations.

The OS, in practice, measures the probability of transition between an initial to a final state. The dipole OS for first two $\ell = 0$ states of WCP, ECSCP, SCP are presented in top, middle and bottom portions of Table III respectively. These changes do not seem to be straight forward. At $\lambda_1 \rightarrow 0$ (WCP) and $\lambda_2 \rightarrow 0$ (ECSCP), these results coalesce to FHA. On the other side, OS in SCP approach FHA in the limit of $r_c \rightarrow \infty$. The selection rule is $\Delta\ell = \pm 1$; therefore, only p-wave states are permitted as final states. In all three occasions, these are provided for $ns \rightarrow mp$ ($n = 1, 2; m = 2, 3$) states, in both *free* and *confined* conditions. In the *first two* plasma conditions, $f_{1s \rightarrow 2p}^{(1)}$ lowers at strong confinement regime ($r_c \leq 1$), with rise in screening constant, keeping r_c fixed. But in low-moderate r_c (1, 2) it increases with λ . However, at $r_c = 5$, it reduces to attain a minimum and then grows gradually. Interestingly, in free condition, it again declines with advancement of λ . On the other hand, in either of the plasmas, at a fixed λ , it increases with r_c , then reaches a maximum and eventually falls off. The positions of the maxima do not change with λ .

TABLE IV: $\alpha^{(1)}$ for WCP, ECSCP (in free and confined conditions) and SCP in $1s$ and $2s$ states.

State	Confined WCP							Free WCP	
	λ_1	$r_c = 0.1$	$r_c = 0.5$	$r_c = 1$	$r_c = 2$	$r_c = 3$	$r_c = 5$	λ_1	$r_c = \infty$
$1s$	0.1	0.00000348	0.00179958	0.02141842	0.14911950	0.25573621	0.28428984	0.05	0.2820913
	0.5	0.00000348	0.00180142	0.02159981	0.15905913	0.29929691	0.35670443	0.1	0.2845122
	1	0.00000348	0.00180662	0.02207243	0.18422797	0.43081698	0.66907982	0.2	0.2937360
	2	0.00000348	0.00182404	0.02347293	0.25795381	0.96822978	4.64009044	0.25	0.3004862
	2.5	0.00000348	0.00183517	0.02427643	0.29812432	1.30252206	8.89513209	0.3	0.3086925
	3	0.00000348	0.00184738	0.02509476	0.33616289	1.60942186	12.66519620	0.4	0.3297730
$2s$	0.1	0.000000784	0.00027589	-0.00105258	-0.30696765	-4.32610957	-150.21895140	0.05	4035.9536
	0.5	0.000000784	0.00027635	-0.00105258	-0.30187923	-4.62797003	503.53816745	0.1	1161.9265
	1	0.000000784	0.00027768	-0.00081299	-0.27873557	-4.40335922	287.82230501	0.2	419.04688
	2	0.000000784	0.00028251	-0.00020805	-0.19039680	-2.24216995	-53.18407330	0.25	339.24125
	2.5	0.000000784	0.00028579	0.00017337	-0.14358283	-1.42113266	-18.92337897	0.3	312.66238
	3	0.000000784	0.00028955	0.00058151	-0.10232148	-0.87783191	-8.40883662	0.4	393.94908
State	Confined ECSCP							Free ECSCP	
	λ_2	$r_c = 0.1$	$r_c = 0.5$	$r_c = 1$	$r_c = 2$	$r_c = 3$	$r_c = 5$	λ_2	$r_c = \infty$
$1s$	0.1	0.00000348	0.00179950	0.02141041	0.14867869	0.25393187	0.28156914	0.01	0.2812505
	0.5	0.00000348	0.00179980	0.02146640	0.15382762	0.28118411	0.33101794	0.05	0.2813193
	1	0.00000348	0.00180171	0.02178057	0.18029000	0.45239114	0.91168796	0.1	0.2817742
	1.25	0.00000348	0.00180359	0.02206630	0.20378040	0.65045235	2.57374006	0.2	0.2850410
	1.4	0.00000348	0.00180507	0.02227983	0.22117395	0.81774044	4.89195099	0.25	0.2883457
$2s$	0.1	0.00000078	0.00027587	-0.00105523	-0.30712416	-4.30664314	-136.34737101	0.01	89914.38
	0.5	0.00000078	0.00027591	-0.00104609	-0.30960540	-4.85239904	230.50804606	0.05	20470.3544
	1	0.00000078	0.00027620	-0.00098316	-0.30418590	-5.36027549	171.45198632	0.1	2954.0860
	1.25	0.00000078	0.00027650	-0.00091626	-0.28685821	-4.42905058	-831.87504495	0.2	546.52109
	1.4	0.00000078	0.00027674	-0.00086180	-0.27036124	-3.63524261	-91.86677448	0.25	386.92234
SCP									
State	$r_c = 0.1$	$r_c = 0.2$	$r_c = 0.5$	$r_c = 1$	$r_c = 2$	$r_c = 2.5$	$r_c = 3$	$r_c = 5$	$r_c = 10$
$1s$	0.00000349	0.00005369	0.00183246	0.022259	0.160406	0.232152	0.273467	0.288320	0.282136
$2s$	0.00000078	0.00001131	0.00028033	0.011415	0.133172	0.275261	0.486354	2.354053	8.230057

In SCP also, $f_{1s \rightarrow 2p}^{(1)}$ imprints a similar behavior; initially gains to reach a maximum and then declines. It can thus be stated that, in all these three plasmas, there is an optimum T (refer to Sec. II.C) at which the probability of transition attains a maximum. Moreover, with growth in r_c and T , the plasma tail effect predominates. At $r_c = 0.1$ and 0.5 , only minor changes occur in $f_{1s \rightarrow 3p}^{(1)}$ with progress in λ , in both WCP and ECSCP. However, at $r_c = 1$, though the values are significantly small, but nevertheless there appears a minimum in $f_{1s \rightarrow 3p}^{(1)}$ versus λ plots, in both plasmas. At $r_c = 2$, it decays with growth in λ . Further, at $r_c = 5$, there appears a maximum in $f_{1s \rightarrow 3p}^{(1)}$ against λ_2 plot in ECSCP. However, in the

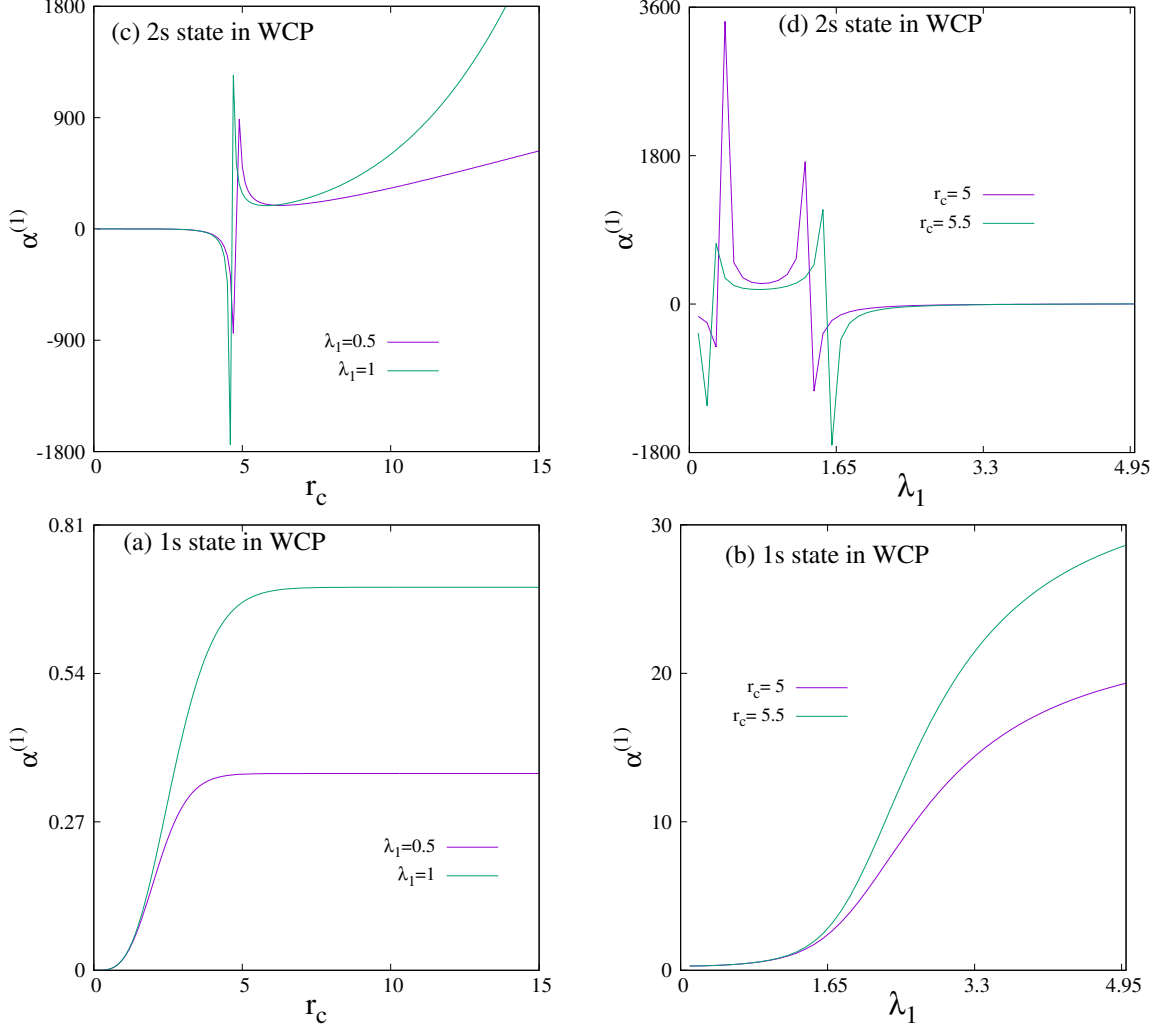


FIG. 6: $\alpha^{(1)}$ in 1s, 2s states in WCP. In panels (a)-(b), r_c variation at two selected λ_1 (0.5, 1), and in panels (c)-(d), λ_1 variation at two different r_c (5, 5.5). See text for details.

similar plot for WCP, one finds a maximum followed by a minimum. On the contrary, at a fixed λ , in WCP and ECSCP with rise in r_c , $f_{1s \rightarrow 3p}^{(1)}$ decreases to reach a minimum and then increases. But in SCP, at first, there occurs a minimum followed by a maximum. Thus, with rise in T , the probability of transition from 1s to 3p decreases initially in all these three potentials, and increases thereafter. It is noticed that, $f_{1s \rightarrow mp}^{(1)} (m = 2, 3)$ in *free* WCP and ECSCP reduces with progress in λ .

Now, the focus is on 2s states. Like the previous case, here also non-trivial variations are recorded in their changes with r_c and λ . In this case, the occurrence of a negative sign in $f_{2s \rightarrow 2p}^{(1)}$ indicates emission. In WCP and ECSCP, at a fixed r_c in strong confinement region ($r_c \leq 2$), it remains almost unchanged with changes in λ . At this low r_c region, emission

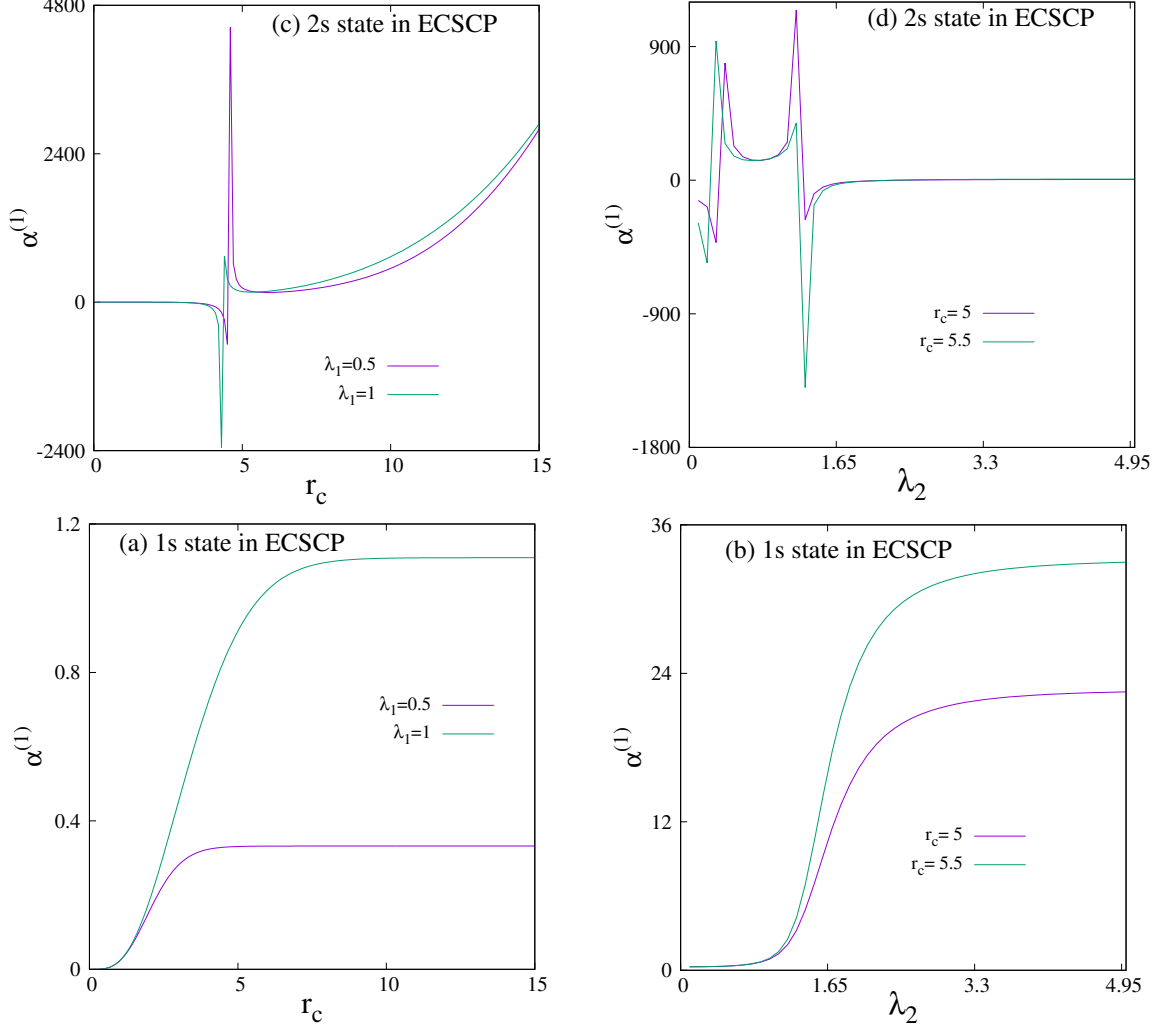


FIG. 7: $\alpha^{(1)}$ for ECSCP in 1s and 2s states. Panels (a)-(b): r_c variation at two selected λ_1 (0.5, 1); panels (c)-(d): λ_1 variation at two different r_c (5, 5.5). See text for details.

occurs between these two states for all the λ considered. However, in $r_c = 5$, emission happens at lower values of λ . Thus, at this particular r_c , there appears a crossover between \mathcal{E}_{2s} and \mathcal{E}_{2p} , with progress in λ . The 2s to 3p transition provides absorption spectrum. Similar to $f_{2s \rightarrow 2p}^{(1)}$, at strong confinement zone (at a fixed r_c), nominal changes occur in $f_{2s \rightarrow 3p}^{(1)}$ in both WCP and ECSCP. The same, however, at $r_c = 5$, decreases with rise in λ . At a fixed λ , with rise in r_c , it advances to reach a maximum and then decays. Similarly, in SCP also, one gets a maximum with increase in r_c , at fixed λ . One observes that, in both WCP and ECSCP, $f_{2s \rightarrow mp}^{(1)}(m = 2, 3)$ decays with growth in λ . The above results of Table III are graphically shown in Figs. IV and V for *confined WCP* and *confined ECSCP* respectively. Thus $f_{ns \rightarrow 2p}^{(1)}(n = 1, 2)$ is plotted as function of (a) r_c at fixed λ and (b) λ at

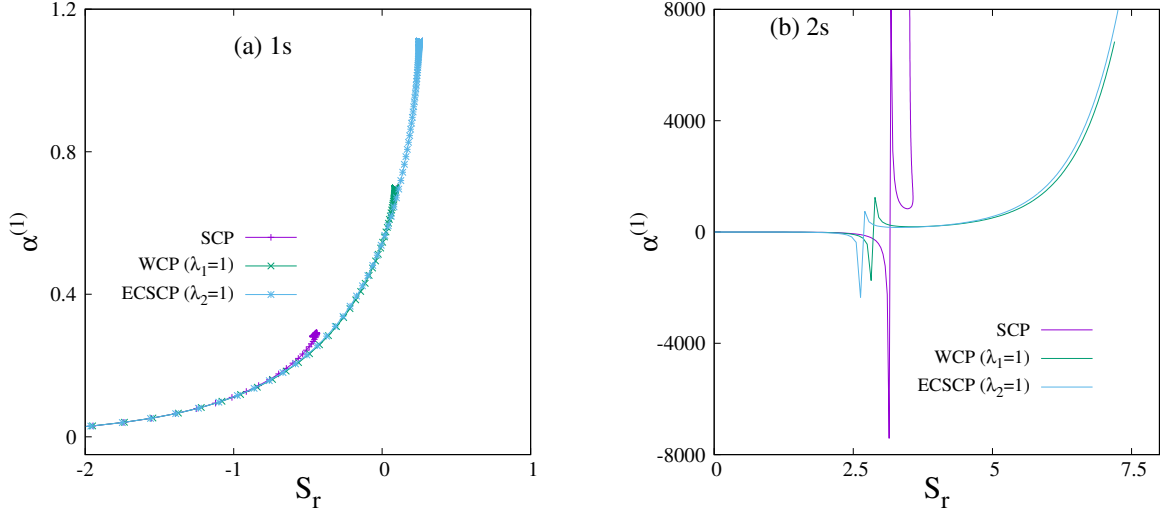


FIG. 8: Change in $\alpha^{(1)}$ with S_r in SCP, WCP ($\lambda_1 = 1$), ECSCP ($\lambda_2=1$) involving (a) $1s$ and (b) $2s$ states. See text for details.

given r_c in these plasma conditions. Two representative λ (5, 10) and r_c (0.1, 0.5) are chosen to illustrate these. There are certain similarities in the qualitative nature of these plots in two left panels, (a) of Figs. IV and V, as well as two right panels, (b). From panels (a) of these figures, one notices that, for both λ values, starting from a non-zero positive number, $f_{1s \rightarrow 2p}^{(1)}$ grows to a moderate extent, to reach a maximum at a lower r_c , and then sharply falls until converging to the respective free system. However, $f_{2s \rightarrow 2p}^{(1)}$ starts from a small negative number, then lowers to a slight extent to attain a minimum, and finally accelerates rapidly to reach the corresponding free limit, in both WCP and ECSCP (also shown in left panels). Next, panels (b) shows, $f_{1s \rightarrow 2p}^{(1)}$ gradually falls to a minimum from an initial positive number with progress in λ and thereafter grows until arriving at the free limit. As r_c progresses, the plots display a well-like behavior with a flatter minimum, without any significant change in the positions of these minima. On the other hand, $f_{2s \rightarrow 2p}^{(1)}$ (again from panel (b)), initially shows a tendency to reach a maximum (which flattens with rise in r_c) followed by a sharp fall to attain the FHA limit. All these patterns are not necessarily evident from the table, as it offers only few entries to minimize the space. Thus one sees that $1s$ and $2s$ states maintain a complementary nature in Figs. IV and V.

Now, Table IV presents dipole polarizabilities, $\alpha^{(1)}$, in $1s$ and $2s$ for all the three plasmas. It retains the arrangement pattern of Table III; so the top, middle and bottom portion contain results of WCP, ECSCP and SCP respectively. However, the chosen λ 's differ from Table III. At lower r_c 's (≤ 0.5) covered, $\alpha_{ns}^{(1)}$ is quite small and remains practically unaltered

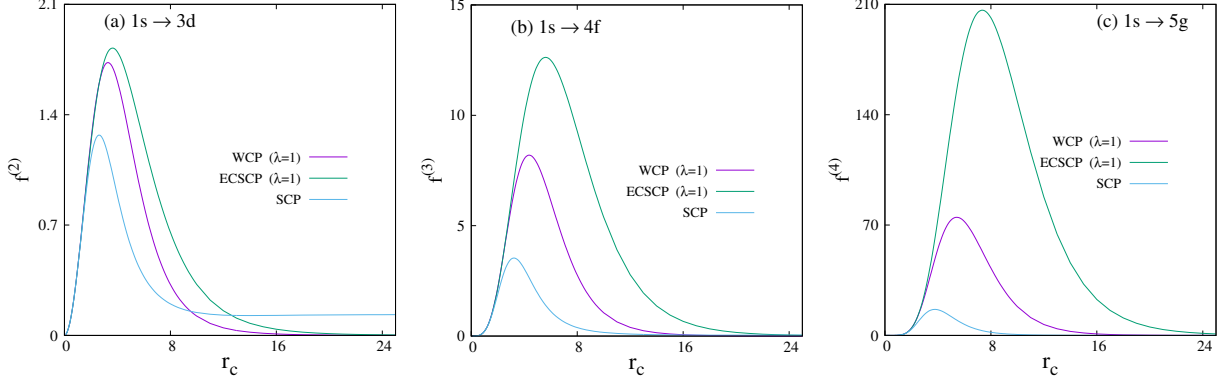


FIG. 9: Changes in (a) $f_{(1s \rightarrow 3d)}^{(2)}$ (b) $f_{(1s \rightarrow 4f)}^{(3)}$ and (c) $f_{(1s \rightarrow 5g)}^{(4)}$ with r_c , in WCP ($\lambda_1 = 1$), ECSCP ($\lambda_2=1$) and SCP. See text for details.

with changes in λ . Similarly, in SCP also, it is rather small. In $r_c > 0.5$ region, however, $\alpha_{1s}^{(1)}$ continually increases with λ , for a fixed r_c . Further, at a specific λ , it progresses with r_c . In essence, it is concluded that, in $1s$ state, with relaxation in confinement (increase in T) $\alpha^{(1)}$ enhances. However, in $2s$ state, $\alpha^{(1)}$ does not maintain the regular feature of ground state. Thus, $\alpha_{2s}^{(1)}$ at $r_c = 0.5$ is higher compared to its counterpart in $r_c = 0.1$, for all λ 's. In WCP and ECSCP, it progresses with λ at a constant r_c . At $r_c = 1$, in WCP $\alpha_{2s}^{(1)}$ attains (-)ve value at lower λ_1 ; with rise in λ_1 it generally grows and eventually becomes (+)ve towards the end. In contrast, in ECSCP it remains (-)ve for all the λ_2 considered, and slowly increases as we descend down the column. Further, at $r_c = 2, 3$, in both WCP and ECSCP, it reflects (-)ve value but, overall, advances with rise in λ . Interestingly, however, at $r_c = 5$, in either WCP or ECSCP, it starts from an initial (-)ve value at lower λ , then escalates to a (+)ve, followed by a drop to attain certain (-)ve value again. These results have prompted us to investigate the behavior of $\alpha_{ns}^{(1)}$ as function of λ , keeping r_c fixed at 5 and 5.5 in their corresponding plots (see Figs. 6 and 7, later). However, in SCP, $\alpha_{ns}^{(1)}$ smoothly increases from a small number to reach a maximum and finally merge to FHA results (0.282136 and 7.5002 for $1s$ and $2s$). In free WCP and ECSCP, $\alpha_{1s}^{(1)}$ accelerates while $\alpha_{2s}^{(1)}$ reduces with growth in λ . These are demonstrated in the last two columns.

The above $\alpha_{ns}^{(1)}$ results of Table IV are depicted graphically in Figs. 6 and 7. Thus two lower left panels (a) suggest that, at a fixed λ (0.5, 1), $\alpha_{1s}^{(1)}$ steadily progresses with r_c until converging to free limit. The two lower right panels (b) show that, at fixed r_c (5, 5.5), $\alpha_{1s}^{(1)}$ advances, initially slowly, but later sharply with λ , and then reach the FHA limit. It is observed that, in either WCP or ECSCP, the numerical value of $\alpha_{1s}^{(1)}$ at $r_c = 5.5$ remains

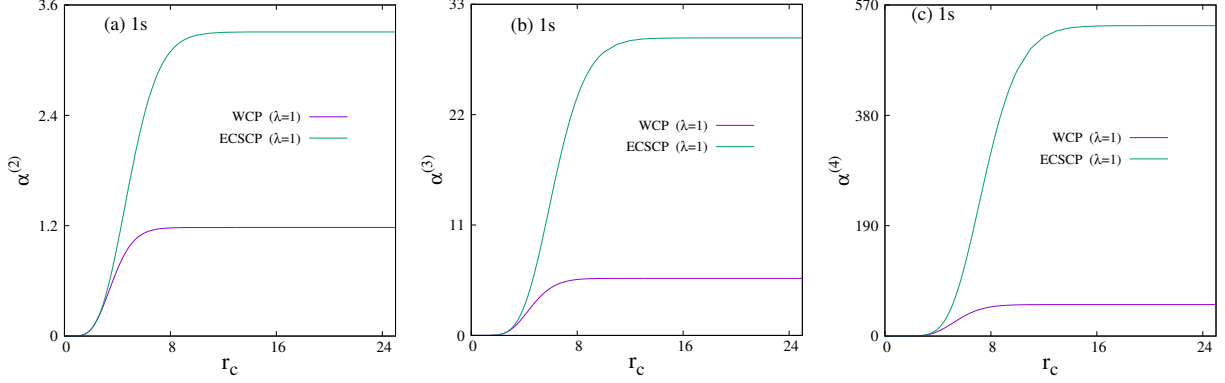


FIG. 10: Changes in (a) $\alpha^{(2)}$ (b) $\alpha^{(3)}$ and (c) $\alpha^{(4)}$, with r_c , involving $1s$ state of WCP ($\lambda_1 = 1$) and ECSCP ($\lambda_2=1$). See text for details.

higher compared to that at $r_c = 5$. Similarly, the top rows of these figures provide respective plots for $2s$ in WCP and ECSCP. From two lower right panels (c), it is inferred that, for a given λ (0.5, 1), $\alpha_{2s}^{(1)}$ records some abrupt fall to a high (-)ve at certain r_c , followed by a dramatic shoot-up to a high (+)ve in a spike-like fashion, then again a drop and eventually steady growth, thus giving rise to one maximum and minimum. On the contrary, at $r_c = 5$ or 5.5, in two top right panels (d), it proceeds through two spike-like features with change of sign in between high (-)ve to high (+)ve, passing through two maxima and minima. This complex pattern may occur due to a sign change in various energy states.

From the above discussion it appears that, the impact of confinement on $\alpha_{ns}^{(1)}$ ($n = 1, 2$) is thought provoking. In order to probe it further, it would be interesting to invoke Shannon entropy. It is well known that, S_r is an efficient measure of confinement [67, 69]; with increase of confinement strength S_r decreases, while enhancing with its relaxation. Therefore $\alpha^{(1)}$ has been plotted as function of S_r in both $1s, 2s$ states of all these three plasmas. In WCP and ECSCP λ is kept fixed at 1. Panel (a) in Fig. 8 signifies that, in all these three occasions, $\alpha_{1s}^{(1)}$ progress with S_r . But the same for $2s$ in panel (b) shows a behavior that is not so straightforward. Therefore an in-depth analysis would be highly desirable.

At last, some sample results are now presented for quadrupole, octupole and hexadecapole OS, as well as the polarizabilities involving WCP, ECSCP and SCP. The selection rules for these three different transitions are $\Delta\ell \pm 2, 3$ and 4 respectively. To illustrate the qualitative features, we offer a cross section of these, while detailed results will be published elsewhere. Figure 9 imprints the variation of $f^{(2)}, f^{(3)}, f^{(4)}$ respectively, as function of r_c , for the three potentials, in panels (a)-(c), for $1s \rightarrow 3d$, $1s \rightarrow 4f$ and $1s \rightarrow 5g$ transitions. In WCP

and ECSCP λ was chosen to be 1. For all three potentials, OS rises with r_c , then attains a maximum and finally reach the free values. This features holds true for all the higher order OS. That means, there exists a characteristic r_c at which the probability of concerned transition is maximum. Similarly, the left, middle and right panels of Fig. 10 displays changes in $\alpha^{(2)}, \alpha^{(3)}, \alpha^{(4)}$, with r_c in $1s$ state for WCP and ECSCP. In both plasmas, $\alpha^{(k)}$ continually increases until reaching a constant value corresponding to the free system. The analogous SCP plots are qualitatively similar, and thus omitted.

IV. CONCLUSION

Multipole (up to order 4) OS and polarizabilities are probed for H-like ions in WCP, ECSCP and SCP. In first two cases, investigation is done in both *free* and *confined* conditions. The connection between T and r_c is proposed and analyzed. It is found that, the plasma tail effect can be controlled by introducing this confinement. Two generalized scaling ideas are derived connecting Z and λ separately. The relation between these two independent ideas is also achieved. Starting from a given Hamiltonian and using these designed relations, one can easily extract results for a series of Hamiltonian. A new S_r -driven technique is designed to determine $\lambda_{n,\ell}^{(c)}$ for both WCP and ECSCP in free environment accurately, where it shoots up stiffly. Further, using S_r -based results, and this scaling idea, a generalized relation between $\lambda_{n,\ell}^{(c)}$ and Z is proposed, which is applicable to an arbitrary state. The applicability of a recently proposed virial-like theorem has been verified to the plasma systems studied here. Results are also presented in *free* WCP and ECSCP. A detailed investigation of these spectroscopic properties for $\ell \neq 0$ states would be highly desirable. The influence of plasma screening effect on two-photon transition amplitude, photoionization cross section also need to be explored in confined condition. Other information-theoretic quantities like Fisher information, Onicescu energy, complexity, mutual and relative information, etc., are required to be examined. Exploration of Hellmann-Feynman theorem in the context of *confined* plasma is necessary. Similar calculation in Helium plasmas may provide vital insight about the effect of confinement on many-electron plasmas.

V. ACKNOWLEDGEMENT

Financial support from BRNS, India (sanction order: 58/14/03/2019-BRNS/10255) is gratefully acknowledged. NM thanks CSIR, New Delhi, India, for a Senior Research Associateship (Pool No. 9033A).

Appendix A: Analytical forms of $f^{(k)}$ and $\alpha^{(k)}$ in FHA

Analytical expression of dipole polarizabilities in FHA was reported in [70] for $1s$ state. In this appendix, we provide the 2^k -pole OS ($k = 1, 4$) and respective polarizabilities for FHA, in both $1s, 2s$ states.

The closed form expressions of $f_{(1s \rightarrow np)}^{(1)}(Z)$ and $f_{(2s \rightarrow np)}^{(1)}(Z)$ are obtained as,

$$\begin{aligned} f_{(1s \rightarrow np)}^{(1)}(Z) &= \frac{2^8}{3Z^7} n^5 \frac{(n-1)^{(2n-4)}}{(n+1)^{(2n+4)}}, \\ f_{(2s \rightarrow np)}^{(1)}(Z) &= \frac{2^{15}}{3Z^7} n^5 (n^2 - 1) \frac{(n-2)^{(2n-5)}}{(n+2)^{(2n+5)}}. \end{aligned} \quad (\text{A1})$$

Now, applying Eq. (A1) in Eq. (7), one easily obtains $\alpha_i^{(1)}(\text{bound})(Z)$ for $1s$ and $2s$ states of FHA. They take the following forms,

$$\begin{aligned} \alpha_{1s}^{(1)}(\text{bound})(Z) &= \sum_{i=2}^n \frac{2^{10}}{3Z^9} i^9 \frac{(i-1)^{(2i-6)}}{(i+1)^{(2i+6)}}, \\ \alpha_{2s}^{(1)}(\text{bound})(Z) &= \sum_{i=2}^n \frac{2^{21}}{3Z^9} i^9 (i^2 - 1) \frac{(i-2)^{(2i-7)}}{(i+2)^{(2i+7)}}. \end{aligned} \quad (\text{A2})$$

$f_{(1s \rightarrow nd)}^{(2)}(Z)$ and $f_{(2s \rightarrow nd)}^{(2)}(Z)$ are expressed as,

$$\begin{aligned} f_{(1s \rightarrow nd)}^{(2)}(Z) &= \frac{2^{12}}{5Z^9} n^7 (n^2 - 4) \frac{(n-1)^{(2n-6)}}{(n+1)^{(2n+6)}}, \\ f_{(2s \rightarrow nd)}^{(2)}(Z) &= \frac{2^{27}}{5Z^9} n^7 (n^2 - 1) \frac{(n-2)^{(2n-9)}}{(n+2)^{(2n+9)}}. \end{aligned} \quad (\text{A3})$$

Invoking Eq. (A3) in Eq. (7), one gets $\alpha_i^{(2)}(\text{bound})(Z)$ in $1s$ and $2s$ states of FHA as follows,

$$\begin{aligned} \alpha_{1s}^{(2)}(\text{bound})(Z) &= \sum_{i=3}^n \frac{2^{12}}{5Z^{11}} i^{11} (i^2 - 4) \frac{(i-1)^{(2i-8)}}{(i+1)^{(2i+8)}}, \\ \alpha_{2s}^{(2)}(\text{bound})(Z) &= \sum_{i=3}^n \frac{2^{33}}{5Z^{11}} i^{11} (i^2 - 1) \frac{(i-2)^{(2i-10)}}{(i+2)^{(2i+10)}}. \end{aligned} \quad (\text{A4})$$

The analytical expressions for $f_{(1s \rightarrow nf)}^{(3)}(Z)$ and $f_{(2s \rightarrow nf)}^{(3)}(Z)$ are presented as,

$$\begin{aligned} f_{(1s \rightarrow nf)}^{(3)}(Z) &= \frac{9}{7} \frac{2^{12}}{Z^{11}} n^9 (n^2 - 9)(n^2 - 4) \frac{(n - 1)^{(2n-8)}}{(n + 1)^{(2n+8)}}, \\ f_{(2s \rightarrow nf)}^{(3)}(Z) &= \frac{9}{7} \frac{2^{27}}{5Z^{11}} n^9 (n^2 - 9)(n^2 + 4)(n^2 - 1) \frac{(n - 2)^{(2n-10)}}{(n + 2)^{(2n+10)}}. \end{aligned} \quad (\text{A5})$$

Doing some mathematical manipulation after substituting Eq. (A5) in Eq. (7), yields $\alpha_i^{(3)}(\text{bound})(Z)$ for $1s$ and $2s$ states of FHA as below,

$$\begin{aligned} \alpha_{1s}^{(3)}(\text{bound})(Z) &= \sum_{i=4}^n \frac{9}{7} \frac{2^{14}}{Z^{13}} i^{13} (i^2 - 9)(i^2 - 4) \frac{(i - 1)^{(2i-10)}}{(i + 1)^{(2i+10)}}, \\ \alpha_{2s}^{(3)}(\text{bound})(Z) &= \sum_{i=4}^n \frac{9}{7} \frac{2^{33}}{Z^{13}} i^{13} (i^2 - 9)(i^4 + 4)(i^2 - 1) \frac{(i - 2)^{(2i-12)}}{(i + 2)^{(2i+12)}}. \end{aligned} \quad (\text{A6})$$

Finally, $f_{(1s \rightarrow ng)}^{(4)}(Z)$ and $f_{(2s \rightarrow ng)}^{(4)}(Z)$ are manifested as,

$$\begin{aligned} f_{(1s \rightarrow ng)}^{(4)}(Z) &= \frac{2^{18}}{9Z^{13}} n^{11} (n^2 - 16)(n^2 - 9)(n^2 - 4) \frac{(n - 1)^{(2n-10)}}{(n + 1)^{(2n+10)}}, \\ f_{(2s \rightarrow ng)}^{(4)}(Z) &= \frac{2^{39}}{9Z^{13}} n^{11} (n^2 - 16)(n^2 - 9)(n^2 + 2)^2(n^2 - 1) \frac{(n - 2)^{(2n-12)}}{(n + 2)^{(2n+12)}}. \end{aligned} \quad (\text{A7})$$

By replacing Eq. (A7) in Eq. (7) one may extract $\alpha_i^{(4)}(\text{bound})(Z)$ for $1s, 2s$ with the form,

$$\begin{aligned} \alpha_{1s}^{(4)}(\text{bound})(Z) &= \sum_{i=5}^n \frac{2^{20}}{9Z^{15}} i^{15} (i^2 - 16)(i^2 - 9)(i^2 - 4) \frac{(i - 1)^{(2i-12)}}{(i + 1)^{(2i+12)}}, \\ \alpha_{2s}^{(4)}(\text{bound})(Z) &= \sum_{i=5}^n \frac{2^{45}}{9Z^{15}} i^{15} (i^2 - 16)(i^2 - 9)(i^2 + 2)^2(i^2 - 1) \frac{(i - 2)^{(2i-14)}}{(i + 2)^{(2i+14)}}. \end{aligned} \quad (\text{A8})$$

Appendix B: Some selected results using scaling concept

Here, we demonstrate the derived relations presented in Sec.II.D. Table V, imprints some sample results obtained by the proposed scaling concept. Here, we have used these formulas to connect Z , λ and r_c . However, it can be applied and extended to any Hamiltonian.

The top, middle and bottom portions present results for WCP, ECSCP and SCP respectively. In all three cases, columns $\{2, 3\}, \{6, 7\}, \{10, 11\}$ and $\{4, 5\}, \{8, 9\}, \{12, 13\}$ form two separate groups. Here, due to lack of space, we restrict our calculation using three Hamiltonians. However, one can extend the number of such Hamiltonians in a given group by using this formulation. Interestingly, one can extract the results for all members of a

TABLE V: $\mathcal{E}_{n,0}, f_{ns \rightarrow 2p}^{(1)}, \alpha_{ns}^{(1)}$ ($n = 1, 2$) values for three Hamiltonians, given in Eqs. (44).

WCP												
	$H\left(1, 1, \frac{\lambda_1}{Z}, Zr_c, r_1\right)$				$H\left(1, \frac{Z}{\lambda_1}, 1, \lambda_1 r_c, r_2\right)$				$H\left(1, Z, \lambda_1, r_c, r\right)$			
$\frac{\lambda_1}{Z}=2$	$H\left(1, 1, 2, 1, r_1\right)$		$H\left(1, 1, 2, 2, r_1\right)$		$H\left(1, 0.5, 1, 2, r_2\right)$		$H\left(1, 0.5, 1, 4, r_2\right)$		$H\left(1, 1, 2, 1, r\right)$		$H\left(1, 2, 4, 1, r\right)$	
$r_c = 1$	$\lambda_1 = 2$	$Z = 1$	$\lambda_1 = 4$	$Z = 2$	$\lambda_1 = 2$	$Z = 1$	$\lambda_1 = 4$	$Z = 2$	$\lambda_1 = 2$	$Z = 1$	$\lambda_1 = 4$	$Z = 2$
	I	II	I	II	I	II	I	II	I	II	I	II
$\mathcal{E}_{1,0}$	3.6923	3.6923	0.8644	0.8644	0.9230	0.9230	0.2161	0.2161	3.6923	3.6923	3.4576	3.4576
$f_{1s \rightarrow 2p}^{(1)}$	0.9825	0.9825	0.9877	0.9877	0.9825	0.9825	0.9877	0.9877	0.9825	0.9825	0.9877	0.9877
$\alpha_{1s}^{(1)}$	0.02998	0.02998	0.42689	0.42689	0.47968	0.47968	6.83026	6.83026	0.02998	0.02998	0.02668	0.02668
$\mathcal{E}_{2,0}$	17.8794	17.8794	4.2884	4.2884	4.4698	4.4698	1.07212	1.07212	17.8794	17.8794	17.1538	17.1538
$f_{2s \rightarrow 2p}^{(1)}$	-0.6051	-0.6051	-0.6039	-0.6039	-0.6051	-0.6051	-0.6039	-0.6039	-0.6051	-0.6051	-0.6039	-0.6039
$\alpha_{2s}^{(1)}$	0.00477	0.00477	0.02271	0.02271	0.07632	0.07632	0.36349	0.36349	0.00477	0.00477	0.00142	0.00142
ECSCP												
	$H\left(1, 1, \frac{\lambda_1}{Z}, Zr_c, r_1\right)$				$H\left(1, \frac{Z}{\lambda_1}, 1, \lambda_1 r_c, r_2\right)$				$H\left(1, Z, \lambda_1, r_c, r\right)$			
$\frac{\lambda_1}{Z}=2$	$H\left(1, 1, 2, 1, r_1\right)$		$H\left(1, 1, 2, 2, r_1\right)$		$H\left(1, 0.5, 1, 2, r_2\right)$		$H\left(1, 0.5, 1, 4, r_2\right)$		$H\left(1, 1, 2, 1, r\right)$		$H\left(1, 2, 4, 1, r\right)$	
$r_c=1$	$\lambda_1 = 2$	$Z = 1$	$\lambda_1 = 4$	$Z = 2$	$\lambda_1 = 2$	$Z = 1$	$\lambda_1 = 4$	$Z = 2$	$\lambda_1 = 2$	$Z = 1$	$\lambda_1 = 4$	$Z = 2$
	I	II	I	II	I	II	I	II	I	II	I	II
$\mathcal{E}_{1,0}$	4.00195	4.00195	1.07647	1.07647	1.00048	1.00048	0.29612	0.29612	4.00195	4.00195	4.30589	4.30589
$f_{1s \rightarrow 2p}^{(1)}$	0.98265	0.98265	0.98488	0.98488	0.98265	0.98265	0.98488	0.98488	0.98265	0.98265	0.98488	0.98488
$\alpha_{1s}^{(1)}$	0.02998	0.02998	0.46172	0.46172	0.47981	0.47981	7.38750	7.38750	0.02998	0.02998	0.02885	0.02885
$\mathcal{E}_{2,0}$	18.1544	18.1544	4.47386	4.47386	4.53860	4.53860	1.11846	1.11846	18.15440	18.15440	17.89546	17.89546
$f_{2s \rightarrow 2p}^{(1)}$	-0.6047	-0.6047	-0.5971	-0.5971	-0.6047	-0.60477	-0.5971	-0.5971	-0.6047	-0.6047	-0.6047	-0.6047
$\alpha_{2s}^{(1)}$	0.00466	0.00466	0.02914	0.02914	0.07454	0.07454	0.46631	0.46631	0.00466	0.00466	0.00182	0.00182
SCP												
	$H\left(1, 1, \left(\frac{\sigma}{Z}\right)^4, Zr_c, r_1\right)$				$H\left(1, \frac{Z}{\sigma}, 1, \sigma r_c, r_2\right)$				$H\left(1, Z, \sigma^4, r_c, r\right)$			
	$H\left(1, 1, \frac{1}{16}, 2, r_1\right)$		$H\left(1, 1, 1, 3B, r_1\right)$		$H\left(1, 2, 1, 1, r_2\right)$		$H\left(1, 1, 1, 3B, r_2\right)$		$H\left(1, 2, 1, 1, r\right)$		$H\left(1, 3, 3, B, r\right)$	
	$\sigma = 1$	$Z = 2$	$\sigma = 3$	$Z = 3$	$\sigma = 1$	$Z = 2$	$\sigma = 3$	$Z = 3$	$\sigma = 1$	$Z = 2$	$\sigma = 3$	$Z = 3$
	I	II	I	II	I	II	I	II	I	II	I	II
$\mathcal{E}_{1,0}$	0.56979	0.56979	5.64694	5.64694	2.27917	2.27917	5.64694	5.64694	2.27917	2.27917	50.64694	50.64694
$f_{1s \rightarrow 2p}^{(1)}$	0.99067	0.99067	0.98176	0.98176	0.99067	0.99067	0.98176	0.98176	0.99067	0.99067	0.98176	0.98176
$\alpha_{1s}^{(1)}$	0.35614	0.35614	0.01769	0.01769	0.02226	0.02226	0.01769	0.01769	0.02226	0.02226	0.00021	0.00021
$\mathcal{E}_{2,0}$	3.99437	3.99437	24.2876	22.2876	15.97749	15.97749	24.2876	24.2876	15.97749	15.97749	218.5886	218.5886
$f_{2s \rightarrow 2p}^{(1)}$	-0.6097	-0.6097	-0.6048	-0.6048	-0.6097	-0.6097	-0.6048	-0.6048	-0.6097	-0.6097	-0.6048	-0.6048
$\alpha_{2s}^{(1)}$	-0.0149	-0.0149	0.00296	0.00296	-0.0009	-0.0009	0.00296	0.00296	-0.0009	-0.0009	0.000036	0.000036

particular group just by performing calculations for any one Hamiltonian belonging to that group. The symbols have following meanings. Firstly, $\alpha_{ns}^{(1)}$ represents the bound-state polarizability. *I* signifies analytical results obtained by employing (a) Eqs. (24),(30),(35) for $\mathcal{E}_{n,\ell}$, (b) Eqs. (26),(32),(42) for $f_{js \rightarrow np}^{(1)}$, (c) Eqs. (27),(33),(43) for $\alpha_{ns}^{(1)}$. *II* indicates numerical results calculated by using the Hamiltonian directly. And finally, $B = \left(\frac{2}{81}\right)^{\frac{1}{3}}$.

Appendix C: $\lambda_{n,\ell}^{(c)}$ values for higher states in WCP and ECSCP

The critical screening, $\lambda_{n,\ell}^{(c)}$, of WCP and ECSCP for $Z = 1 - 4$, in the $3s, 4s, 4p, 4f, 5s, 5p, 5d, 5f, 5g$ states are produced in Table VI.

-
- [1] K. D. Sen (Ed.). *Electronic Structure of Quantum Confined Atoms and Molecules*. Springer International Publishing, Switzerland, 2014.
 - [2] W. Grochala, R. Hoffmann, J. Feng, and N. W. Ashcroft. *Angew. Chem. Int. Ed.*, 46:3620, 2007.
 - [3] E. Snider, N. Dasenbrock-Gammon, R. McBride, M. Debessai, H. Vindana, K. Vencatasamy, K. V. Lawler, A. Salammat, and R. P. Dias. *Nature*, 586:373, 2020.
 - [4] S. Ichimaru. *Rev. Mod. Phys.*, 54:1017, 1982.
 - [5] J. C. Weisheit. *Advances in Atomic and Molecular Physics*, 25:101, 1989.
 - [6] M. S. Murillo and J. C. Weisheit. *Phys. Rep.*, 302:1, 1998.
 - [7] L. Zhu, Yu. Ying He, L. G. Jiao, Y. C. Wang, and Y. K. Ho. *Phys. Plasmas*, 27:072101, 2020.
 - [8] S. Bhattacharyya, J. K. Saha, and T. K. Mukherjee. *Phys. Rev. A*, 91:042515, 2015.
 - [9] L. G. Jiao, Y. Y. He, Y. Z. Zhang, and Y. K. Ho. *J. Phys. B*, 2021.
 - [10] M. Das. *Phys. Plasmas*, 21:012709, 2014.
 - [11] A. Solyu. *Phys. Plasmas*, 19:072701, 2012.
 - [12] S. Paul and Y. K. Ho. *Phys. Plasmas*, 16:063302, 2009.
 - [13] M. K. Bahar and A. Solyu. *Phys. Plasmas*, 092703:21, 2014.
 - [14] M. K. Bahar, A. Soylyu, and A. Poszwa. *IEEE Trans. Plasma Sci.*, 44:2297, 2016.
 - [15] F. A. Gutierrez and J. Diaz-Valdés. *J. Phys. B*, 27:593, 1994.
 - [16] J.-S. Yoon and Y.-D. Jung. *Phys. Plasmas*, 3:3291, 1996.
 - [17] S. Paul and Y. K. Ho. *Phys. Plasmas*, 15:073301, 2008.
 - [18] S. Paul and Y. K. Ho. *Phys. Rev. A*, 79:032714, 2009.
 - [19] Y.-D. Jung. *Phys. Plasmas*, 332:2, 1995.
 - [20] Y.-D. Jung and J.-S. Yoon. *J. Phys. B*, 29:3549, 1996.
 - [21] M. Y. Song and Y.-D. Jung. *Phys. Plasmas*, 36:2119, 2003.
 - [22] Y.-D. Jung. *Phys. Plasmas*, 4:21, 1997.

TABLE VI: $\lambda_{n,\ell}^{(c)}$ for H-like ions ($Z = 1-4$) for $3s, 4s, 4p, 4f, 5s, 5p, 5d, 5f, 5g$ states in WCP, ECSCP.

WCP				ECSCP			
Z	State	$\lambda_{n,\ell}^{(c)}$	$\mathcal{E}_{n,\ell}$	Z	State	$\lambda_{n,\ell}^{(c)}$	$\mathcal{E}_{n,\ell}$
1	3s	0.13656 [†]	-0.00000013	1	3s	0.289685 [‡]	-0.00000005
2	3s	0.27614	-0.00000013	2	3s	0.217247	-0.00000014
3	3s	0.41563	-0.00000012	3	3s	0.144808	-0.00000026
4	3s	0.55510	-0.00000015	4	3s	0.072366	-0.00000009
1	4s	0.07636 [†]	-0.00000020	1	4s	0.040407 [‡]	-0.00000015
2	4s	0.1554320	-0.00000001	2	4s	0.080838	-0.00000009
3	4s	0.23433	-0.00000002	3	4s	0.121266	-0.00000016
4	4s	0.31319	-0.00000005	4	4s	0.161693	-0.00000077
1	4p	0.06769 [†]	-0.00000058	1	4p	0.03926 [‡]	-0.00000076
2	4p	0.13572	-0.00000025	2	4p	0.078526	-0.00000116
3	4p	0.20363	-0.00000116	3	4p	0.117789	-0.00000025
4	4p	0.271529	-0.00000076	4	4p	0.157053	-0.00000058
1	4f	0.04984 [†]	-0.00000024	1	4f	0.035241 [‡]	-0.00000016
2	4f	0.099662	-0.00000014	2	4f	0.0704820	-0.00000064
3	4f	0.149493	-0.00000031	3	4f	0.1057237	-0.00000005
4	4f	0.193324	-0.00000056	4	4f	0.1409649	-0.00000019
1	5s	0.04822 [†]	-0.00000024	1	5s	0.02578 [‡]	-0.00000016
2	5s	0.09921	-0.00000022	2	5s	0.051569	-0.00000065
3	5s	0.14991	-0.00000006	3	5s	0.077357	-0.00000065
4	5s	0.20054	-0.00000017	4	5s	0.103145	-0.00000024
1	5p	0.04471 [†]	-0.00000001	1	5p	0.025313 [‡]	-0.00000039
2	5p	0.090253	-0.00000007	2	5p	0.05063	-0.00000068
3	5p	0.125506	-0.00000001	3	5p	0.075946	-0.00000083
4	5p	0.18071	-0.00000063	4	5p	0.101262	-0.00000064
1	5d	0.03996 [†]	-0.00000002	1	5d	0.024499 [‡]	-0.00000037
2	5d	0.08004	-0.00000081	2	5d	0.049	-0.00000001
3	5d	0.120072	-0.00000007	3	5d	0.0735	-0.00000006
4	5d	0.160097	-0.00000002	4	5d	0.098	-0.00000010
1	5f	0.03538 [†]	-0.00000055	1	5f	0.023482 [‡]	-0.00000008
2	5f	0.070778	-0.00000023	2	5f	0.046964	-0.00000035
3	5f	0.106168	-0.00000008	3	5f	0.0704464	-0.00000012
4	5f	0.141557	-0.00000038	4	5f	0.0939286	-0.00000006
1	5g	0.031343 [†]	-0.00000006	1	5g	0.022371 [‡]	-0.00000029
2	5g	0.062687	-0.00000007	2	5g	0.0447428	-0.00000007
3	5g	0.09403	-0.00000056	3	5g	0.0671140	-0.00000056
4	5g	0.125374	-0.00000024	4	5g	0.0894856	-0.00000026

[†]Literature results of $\lambda_{n,\ell}^{(c)}$ [51, 66]: (a) $\lambda_{3s}^{(c)} = 0.1394$ (b) $\lambda_{4s}^{(c)} = 0.07882$ (c) $\lambda_{4p}^{(c)} = 0.067885$ (d) $\lambda_{4f}^{(c)} = 0.049831$

(e) $\lambda_{5s}^{(c)} = 0.05058$ (f) $\lambda_{5p}^{(c)} = 0.045186$ (g) $\lambda_{5d}^{(c)} = 0.040024$ (h) $\lambda_{5f}^{(c)} = 0.035389$ (i) $\lambda_{5g}^{(c)} = 0.031343$.

[‡]Literature results of $\lambda_{n,\ell}^{(c)}$ [40, 51, 66]: (a) $\lambda_{3s}^{(c)} = 0.072436$ (b) $\lambda_{4s}^{(c)} = 0.040427$ (c) $\lambda_{4p}^{(c)} = 0.039263$ (d) $\lambda_{4f}^{(c)} = 0.035241$

(e) $\lambda_{5s}^{(c)} = 0.025787$ (f) $\lambda_{5p}^{(c)} = 0.025315$ (g) $\lambda_{5d}^{(c)} = 0.024500$ (h) $\lambda_{5f}^{(c)} = 0.023482$ (i) $\lambda_{5g}^{(c)} = 0.022371$.

- [23] Y. Y. Qi, J. G. Wang, and R. K. Janev. *Phys. Rev. A*, 80:063404, 2009.
- [24] L. Liu and J. G. Wang. *J. Phys. B*, 41:155701, 2008.
- [25] L. Liu, J. G. Wang, and R. K. Janev. *Phys. Rev. A*, 77:042712, 2008.
- [26] A. Poszwa and M. K. Bahar. *Phys. Plasmas*, 22:012104, 2015.
- [27] B. Saha, P. K. Mukherjee, and G. H. F. Diercksen. *Astron. Astrophys.*, 396:337, 2002.
- [28] Y. Y. Qi, J. G. Wang, and R. K. Janev. *Phys. Rev. A*, 78:062511, 2008.
- [29] Y. Y. Qi, Y. Wu, J. G. Wang, and Y. Z. Qu. *Phys. Plasmas*, 16:023502, 2009.
- [30] Y. Y. Qi, J. G. Wang, and R. K. Janev. *Phys. Rev. A*, 80:032502, 2009.
- [31] M. Bassi and K. L. Baluja. *Indian J. Phys.*, 86:961, 2012.
- [32] B. Saha and P. K. Mukherjee. *Phys. Lett. A*, 302:105, 2002.
- [33] M. Das. *Phys. Plasmas*, 19:092707, 2012.
- [34] S. Kang, Y. C. Yang, J. He, F. Q. Xiong, and N. Xu. *Cent. Eur. J. Phys.*, 11:584, 2013.
- [35] J. K. Saha, T. K. Mukherjee, P. K. Mukherjee, and B. Fricke. *Eur. Phys. J. D*, 62:205, 2011.
- [36] H. E. Montgomery Jr., K. D. Sen, and J. Katriel. *Phys. Rev. A*, 97:022503, 2018.
- [37] C. Stubbins. *Phys. Rev. A*, 48:220, 1993.
- [38] C. S. Lam and Y. P. Varshni. *Phys. Rev. A*, 6:1391, 1972.
- [39] C. S. Lai. *Phys. Rev. A*, 26:2245, 1982.
- [40] D. Singh and Y. P. Varshini. *Phys. Rev. A*, 28:2606, 1983.
- [41] R. Dutt, U. Mukherji, and Y. P. Varshini. *J. Phys. B*, 19:3411, 1986.
- [42] O. Bayrak and I. Boztosun. *Int. J. Quant. Chem.*, 107:1040, 2007.
- [43] S. Paul and Y. Ho. *Comput. Phys. Comm.*, 182:130, 2011.
- [44] I. Nasser, M. S. Abdelmonem, and A. Abdel-Hady. *Phys. Scr.*, 84:045001, 2011.
- [45] Y. Y. Qi, J. G. Wang, and R. K. Janev. *Phys. Plasmas*, 23:073302, 2016.
- [46] A. K. Roy. *Int. J. Quant. Chem.*, 113:1503, 2013.
- [47] H. F. Lai, Y. C. Lin, C. Y. Lin, and Y. K. Ho. *Chin. J. Phys.*, 51:73, 2013.
- [48] C. Y. Lin and Y. K. Ho. *Eur. Phys. J. D*, 57:21, 2010.
- [49] C. Y. Lin and Y. K. Ho. *Comp. Phys. Commun.*, 182:125, 2011.
- [50] S. Lumb, S. Lumb, and M. K. Bahar. *Phys. Rev. A*, 90:032505, 2014.
- [51] C. G. Diaz, F. M. Fernández, and E. A. Castro. *J. Phys. A*, 24:2061, 1991.
- [52] A. K. Roy. *Int. J. Quant. Chem.*, 116:953, 2016.
- [53] M. S. Murillo. *Phys. Plasmas*, 11:2964, 2004.

- [54] M. Belkhiri, C. J. Fontes, and M. Poirier. *Phys. Rev. A*, 92:032501, 2015.
- [55] Z.-B. Chen, H.-W. Hu, K. Ma, X.-B. Liu, X.-L. Guo, S. Li, B.-H. Zhu, L. Huang, and K. Wang. *Phys. Plasmas*, 25:032108, 2018.
- [56] D. Salzmänn and H. Szichman. *Phys. Rev. A*, 35:807, 1987.
- [57] Y. Y. Qi, J. G. Wang, and R. K. Janev. *Phys. Plasmas*, 24:062110, 2017.
- [58] S. Sen, P. Mandal, P. K. Mukherjee, and B. Fricke. *Phys. Plasmas*, 20:013505, 2013.
- [59] N. Mukherjee and A. K. Roy. *Phys. Rev. A*, 99:022123, 2019.
- [60] A. K. Roy. *Mod. Phys. Lett. A*, 29:1450104, 2014.
- [61] A. K. Roy. *J. Math. Chem.*, 52:1405, 2014.
- [62] A. K. Roy. *Mod. Phys. Lett. A*, 29:1450042, 2014.
- [63] N. Mukherjee and A. K. Roy. *J. Phys. B*, 53:235002, 2020.
- [64] A. Dalgarno. *Adv. Phys.*, 11:281, 1962.
- [65] A. Ghosal and Y. K. Ho. *Phys. Rev. E*, 81:016403, 2010.
- [66] A. K. Roy. *Int. J. Quant. Chem.*, 16:953, 2016.
- [67] N. Mukherjee and A. K. Roy. *Int. J. Quant. Chem.*, 118:e25596, 2018.
- [68] J. Katriel and H. E. Montgomery Jr. *J. Chem. Phys.*, 137:114109, 2012.
- [69] N. Mukherjee and A. K. Roy. *Adv. Theo. Simul.*, 1:1800090, 2018.
- [70] A. C. Tanner and A. J. Thakkar. *Int. J. Quant. Chem.*, 24:345, 1983.